P－45

活性型ミクログリアの In Vivo イメージング

○鈴木 弘美[1)]，外山 宏[2)]，工藤 元[2)]，簇野健太郎[3)]，小野健治[1)]，
中根正人[2)]，桃崎壮太郎[3)]，加藤隆司[3)]，伊藤健吾[3)]，澤田 誠[1)]
○ Hiromi Suzuki[1)], Hiroshi Toyama[2)], Gen Kudoh[2)], Kentaro Hatano[3)],
Kenji Ono[1)], Masato Nakane[2)], Sohtaro Momosaki[3)], Takashi Kato[3)],
Kengo Itoh[3)] and Makoto Sawada[1)]

藤田保健衛生大学総合医科学研究所[1)]，藤田保健衛生大学放射線科[2)]，
長寿脳科学研究部[3)]

【目的】
アルツハイマー病などの神経変性疾患、脳梗塞、脳腫瘍などの種々の脳疾患ではミクログリアが活性化し疾患部分に集積することから、神経細胞の変性や生存維持に対する関連性が注目されている。ミクログリアが、脳内において休止型から活性型に形態変化すると末梢型ベンゾジアゼピン受容体(PBR)が発現することが知られており、ポジトロン CT(PET)で PBR を画像化すれば、神経変性部分や障害の状態の診断が可能となる。今回我々は、Ethanol Injury モデルを作成して活性化したミクログリアを PBR 製剤と動物用 PET でイメージングを行った。

【方法】
8 週齢雄 Wistar ラット（体重 220ー260g）にペントバルビツール系薬剤を腹腔内注射で麻酔を施し、脳定位固定装置へ使用して頭部を固定した。歯科用ドリルで Bregma より右 2mm 部分に穴を開け、エタノール 8 μl を注入し、線条体部分に傷害部分を作製しモデルとした。脳内に傷害を作製した後、3 日後麻酔下に 1.5T MRI 装置にリストコイルを使用し、T2 強調像を撮像して線条体の障害の程度を評価した。術後 4 日目で麻酔下に、^{11}C-PK11195 12ー41MBq を尾静脈注射し、動物用 PET 装置で 60 分間ダイナミックスキャンを実施した。PBR の定量的評価として、小脳を参照部位とし、線条体の normalized distribution volume (V^*)(min) を算出し、比較した。PET スキャン終了後、ラット脳を灌流し、活性型ミクログリアを免疫染色して、PET による結果と比較した。コントロールとしてエタノールを注入していないラットについても同様に動物用 PET で評価した。

【結果】
エタノールによる損傷が MRI で確認できたラットの注入側では非注入側に比べて、動物用 PET での撮像画像から PBR 結合量を定量的に観察すると有意な増加があることがわかった。また、同動物組織を用いた免疫染色ではエタノール注入側の線条体には活性化した形態を示すミクログリアを多く認め、動物用 PET

の所見と一致していることから、PBR結合の増大は活性型のミクログリアが損傷部位に集積している可能性が示唆された。

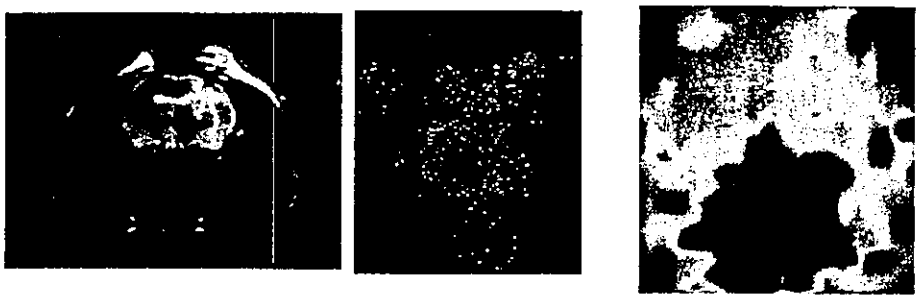

図1　Ethanol InjuryモデルのMRI画像（左）と障害部分に集積したミクログリアの免疫染色（中）とPET画像（右）

【考察】

Ethanol Injury動物モデルにおいて^{11}C-PK11195と動物用PETでPBRを画像化すると、脳内でミクログリアが活性化する状態を評価できることがわかった。ミクログリアはその細胞の性質から脳内で神経変性や細胞障害がある部位に集積して活性化されることが知られている。したがって、PETを用いてPBR結合脳を撮像すれば脳疾患部位の非侵襲的な診断が可能となる。

一方、我々は蛍光標識をしたミクログリアを血管注入した動物に一過性前脳虚血を起こして脳内に進運下ミクログリアの動態を調べたところ、外来性に脳に浸潤したミクログリアは特異的に神経傷害部位に集積することを確認している。一方、ミクログリアは高い貪職能を持つため蛍光マイクロビーズなどの人工物を効率良く取り込み細胞の標識ができる。そこで、脳に導入する前に金属微粒子マグネタイトを取り込ませたミクログリアをラットの頸動脈に注入すると、MRIにより撮像することによって脳の病変部の非侵襲モニタリングにも応用できることも判った。さらに、投与前に細胞に特殊な処理を施すことで神経損傷や脱落を抑制し、神経修復を増強することも明らかになった。この性質を利用すると脳への特異的ドラッグデリバリシステムが構築できるだけでなく、細胞導入によって神経再生、修復が可能となることが考えられる。また、今回のシステムとMRIによる非侵襲モニタリングを組み合わせることによってミクログリアを用いた脳・神経系を標的化した脳疾患の診断や治療の精度や有効性を改善できる可能性があると考えられる。

Plant Cell Physiol. 46(1): 156–165 (2005)
doi:10.1093/pcp/pci008, available online at www.pcp.oupjournals.org
JSPP © 2005

Cell Cycle Dependence of Elicitor-induced Signal Transduction in Tobacco BY-2 Cells

Yasuhiro Kadota [1], Takashi Watanabe [1], Shinsuke Fujii [1], Yutaka Maeda [1], Ryoko Ohno [1], Katsumi Higashi [2], Toshio Sano [3], Shoshi Muto [4,5], Seiichiro Hasezawa [3] and Kazuyuki Kuchitsu [1,2,6]

[1] *Department of Applied Biological Science, Tokyo University of Science, 2641 Yamazaki, Noda, Chiba, 278-8510 Japan*
[2] *Genome & Drug Research Center, Tokyo University of Science, 2641 Yamazaki, Noda, Chiba, 278-8510 Japan*
[3] *Department of Integrated Biosciences, Graduate School of Frontier Sciences, University of Tokyo, Kashiwanoha, Kashiwa, Chiba, 277-8562 Japan*
[4] *Bioscience Center and Graduate School of Bioagricultural Sciences, Nagoya University Chikusa-ku, Nagoya, 464-8610 Japan*

The molecular links between the cell cycle and defense responses in plants are largely unknown. Using synchronized tobacco BY-2 cells, we analyzed the cell cycle dependence of elicitor-induced defense responses. In synchronized cultured apoaequorin-expressing cells, the increase in cytosolic free Ca^{2+} induced by a proteinaceous elicitor, cryptogein, was greatly suppressed during the G_2 and M phases in comparison with G_1 or S phases. Treatment with cryptogein during the G_1 or S phases also induced biphasic (rapid/transient and slow/prolonged) responses in activation of mitogen-activated protein kinases (MAPKs) and production of reactive oxygen species (ROS). In contrast, elicitor treatment during the G_2 or M phases induced only a rapid and transient phase of MAPK activation and ROS production. Their slow and prolonged phases as well as expression of defense-related genes, cell cycle arrest and cell death were induced only after the cell cycle progressed to the G_1 phase; removal of the elicitor before the start of the G_1 phase inhibited these responses. These results suggest that although cryptogein recognition occurred at all phases of the cell cycle, the recognition during the S or G_1 phases, but not at the G_2 or M phases, induces the prolonged activation of MAPKs and the prolonged production of ROS, followed by cell cycle arrest, accumulation of defense-related gene transcripts and cell death. Elicitor signal transduction depends on the cell cycle and is regulated differently at each phase.

Keywords: Cell cycle arrest — Cell death — Elicitor — Synchronized culture — Tobacco BY-2 cells

Abbreviations: $[Ca^{2+}]_{cyt}$, cytosolic free Ca^{2+} concentration; MAPK, mitogen-activated protein kinase; MCLA, 2-methyl-6-[*p*-methoxyphenyl]-3,7-dihydroimidazo[1,2-α]pyrazin-3-one; $^1O_2^-$, superoxide anion radical; ROS, reactive oxygen species; SIPK, salicylic acid-induced protein kinase; WIPK, wounding-induced protein kinase.

Introduction

Plants respond to attack by pathogens by activating a variety of defense mechanisms, including the synthesis of phytoalexins and the induction of hypersensitive cell death, which restricts the growth of pathogens at the infection site (Jones and Dangl 1996, Heath 2000). The induction of defense responses is accompanied by fluxes of Ca^{2+} and H^+, production of reactive oxygen species (ROS) and nitric oxide, and activation of mitogen-activated protein kinases (MAPKs). These responses are thought to have important roles in the induction of defense-related genes and cell death (Zhang and Klessig 2000, Asai et al. 2002, Nürnberger and Scheel 2001, Kadota et al. 2004a).

Down-regulation of cell cycle-related genes is triggered by an oligopeptide elicitor, Pep-13 of *Phytophthora sojae*, in parsley cells (Logemann et al. 1995), implying some links between defense signaling and cell cycle regulation. However, the relationships between the cell cycle and defense responses in plants are unknown. Therefore, we developed a model system involving elicitor-induced hypersensitive cell death in synchronized tobacco BY-2 cells, which we used to analyze the relationship between the cell cycle and defense responses in plants. Since tobacco BY-2 cell suspensions can be synchronized, they have often been used to analyze the mechanisms of cell cycle regulation (Nagata et al. 1992). The proteinaceous elicitor cryptogein, derived from *Phytophthora cryptogea*, induces cell cycle arrest in the G_1 or G_2 phases prior to the induction of cell death (Kadota et al. 2004b). Whether or not cell death is induced is dependent on the stage of the cell cycle at which the elicitor is detected. Cryptogein-induced cell death only occurs in cells in which the elicitor is recognized during the G_1 or S phases, whereas elicitor recognition during the G_2 or M phases does not induce cell death. The inhibition of elicitor-induced cell death during the G_2 or M phases suggests differences in a cryptogein signaling component or components in these phases of the cell cycle.

Cryptogein triggers biphasic transients in the cytosolic free Ca^{2+} concentration ($[Ca^{2+}]_{cyt}$) by plasma membrane Ca^{2+} influx at least partly through the putative Ca^{2+}-permeable channels, NtTPC1s (Kadota et al. 2004c), and Ca^{2+} release from internal Ca^{2+} stores, followed by ROS production (Kadota et al. 2004a) and activation of MAPKs (Zhang et al. 1998) in BY-2 cells. In the present study, using synchronized BY-2 cells, we analyzed the cell cycle dependence of cryptogein signaling

[5] Deceased on January 23, 2004.
[6] Corresponding author: E-mail, kuchitsu@rs.noda.tus.ac.jp; Fax, +81-4-7123-9767.

events in each phase of the cell cycle. Treatment with cryptogein during the G_1 or S phases induced changes in the $[Ca^{2+}]_{cyt}$, a biphasic production of ROS, and a biphasic activation of MAPKs, followed by cell cycle arrest, accumulation of defense-related gene transcripts and cell death. In contrast, treatment during the G_2 or M phases induced much weaker $[Ca^{2+}]_{cyt}$ changes, rapid and transient ROS production and rapid and transient activation of MAPKs, but did not induce the prolonged production of ROS, the prolonged activation of MAPKs, accumulation of defense-related gene transcripts and cell death before cell cycle progression to the G_1 phase. These results suggest that elicitor signaling events including prolonged activation of ROS production and MAPKs that lead to defense gene expression and cell death are regulated in a cell cycle-dependent manner.

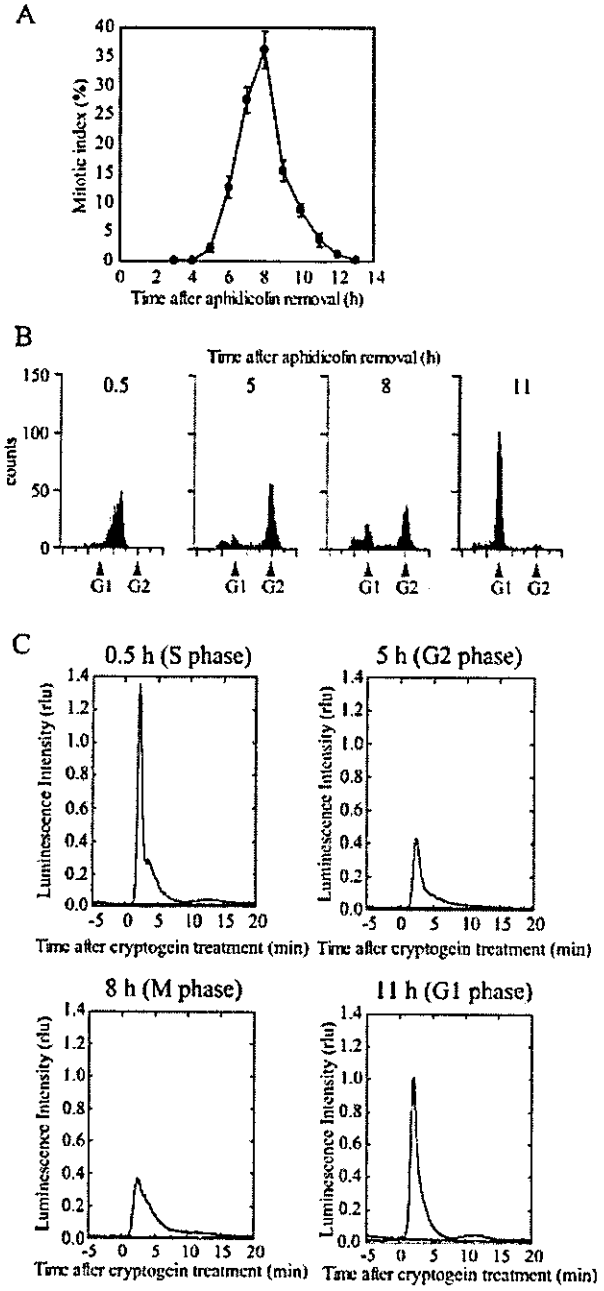

Fig. 1 Cryptogein-induced changes in the $[Ca^{2+}]_{cyt}$ depend on the phase of the cell cycle. BY-2 cells were synchronized at S phase by aphidicolin treatment. (A) Changes in the mitotic index of non-treated cells. The data represent the average of five independent experiments. Error bars indicate the SEM ($n = 5$). (B) Flow cytometric analysis of non-treated cells. Representative results of three independent experiments are shown. (C) Cryptogein (1.5 μM) or distilled water was applied to aequorin-expressing BY-2 cells at 0.5 h (S phase), 5 h (G_2 phase), 8 h (M phase) or 11 h (G_1 phase) after aphidicolin release, and changes in the $[Ca^{2+}]_{cyt}$ were followed by the aequorin luminescence. The peak in the mitotic index was observed 8 h after aphidicolin release (data not shown), suggesting that the progression of the cell cycle was similar to that shown in (A) and (B). The aequorin luminescence curves shown were normalized with the total luminescence of each cell culture. One representative experiment of three independent experiments is shown in each case.

Results

The extent of cryptogein-induced changes in the $[Ca^{2+}]_{cyt}$ depends on the phase of the cell cycle

To analyze the various cryptogein-induced events that occur during the different phases of the cell cycle, the cell cycle of BY-2 cells was synchronized using aphidicolin. The mitotic index of the cells peaked at 8 h after aphidicolin release (Fig. 1A). Flow cytometric analysis showed that almost all of the cells were in the S phase at 0.5 h after aphidicolin release, in the G_2 phase at 5 h after the release and in the G_1 phase at 11 h after the release.

In cultured aequorin-expressing BY-2 cells, the aequorin chemiluminescence is proportional to the $[Ca^{2+}]_{cyt}$ (Takahashi et al. 1997). Cryptogein treatment induces two characteristic transient peaks which correspond to plasma membrane Ca^{2+} influx and inositol 1,4,5-triphosphate-mediated Ca^{2+} release from intracellular Ca^{2+} stores (Kadota et al. 2004a). To examine the cell cycle dependence of the cryptogein-induced changes in the $[Ca^{2+}]_{cyt}$, we analyzed the $[Ca^{2+}]_{cyt}$ during each phase of the cell cycle using synchronized aequorin-expressing cells. The mitotic index of the cells showed a peak at 8 h after aphidicolin release, suggesting that in these cells, cell cycle progression was similar to that of the non-transformed BY-2 cells (data not shown). Aequorin-expressing cells also displayed cryptogein-induced cell cycle arrest, ROS production and cell death that were indistinguishable from the same events in the non-transformed control (data not shown). Cryptogein-induced increases in the $[Ca^{2+}]_{cyt}$ occurred during all phases of the cell cycle, suggesting that the recognition of cryptogein occurred at all phases of the cell cycle. However, the increases that occurred in the G_2 or M phases were much weaker than those in the G_1 or S phases (Fig. 1C). These results suggest that the extent of the cryptogein-induced increase in the $[Ca^{2+}]_{cyt}$ depends on the phase of the cell cycle. Unlike random cultured

cells, the two phases in the $[Ca^{2+}]_{cyt}$ increase were rarely distinguished in synchronized cultured cells for unknown reasons. The shape of the aequorin luminescence trace in the S phase (Fig. 1C) suggests that the two peaks may overlap.

The slow and prolonged activation of MAPKs depends on the phase of the cell cycle during which cryptogein recognition occurs

Treatment of tobacco cell suspensions with cryptogein was shown previously to induce the rapid activation of MAPK homologs with apparent molecular masses of 48 and 44 kDa, corresponding to salicylic acid-induced protein kinase (SIPK) and wounding-induced protein kinase (WIPK), respectively (Lebrun-Garcia et al. 1998, Zhang et al. 1998). To examine the cell cycle dependence of cryptogein-induced activation of protein kinases, protein extracts from cells treated with the elicitor during each phase of the cell cycle were analyzed for kinase activity using an in-gel kinase assay. Treatment with cryptogein during the S or G_1 phases activated p48 and p44 protein kinases (Fig. 2). The activation of p48 protein kinase was biphasic, in that rapid and transient activation occurred at 10 min, and a slow and prolonged activation continued for at least 300 min. The pattern of activation of p44 protein kinase was similar to that of p48 protein kinase; a rapid and transient activation and a slow and prolonged activation. In contrast, treatment with the elicitor during the G_2 or M phases induced rapid and transient activation, followed by rapid inactivation of both kinases. Later, both kinases were reactivated at 300 min (10 h after aphidicolin release) after cryptogein application in the G_2 phase, and at 180 min (11 h after aphidicolin release) and 300 min (13 h after aphidicolin release) after cryptogein application in the M phase. Fig. 1A, B shows that the cells enter the G_1 phase at around 10 h after aphidicolin release, suggesting that the reactivation of MAPKs is well correlated with the progression of the cell cycle to the G_1 phase. Although the rapid and transient activation of p48 protein kinase and the slow and prolonged activation of p44 and p48 protein kinases occurred in all experiments, the rapid and transient activation of p44 protein kinase was not detected in some experiments (data not shown). The washing of cells by extensive growth medium to remove aphidicolin might affect the rapid and transient activation of p44 protein kinase, because wounding stress induces the expression of WIPK (Seo et al. 1995).

In summary, the cryptogein-induced rapid and transient activation of MAPKs occurred when cryptogein was recognized during any of the phases of the cell cycle, but the slow and prolonged activation occurred at the S or G_1 phases.

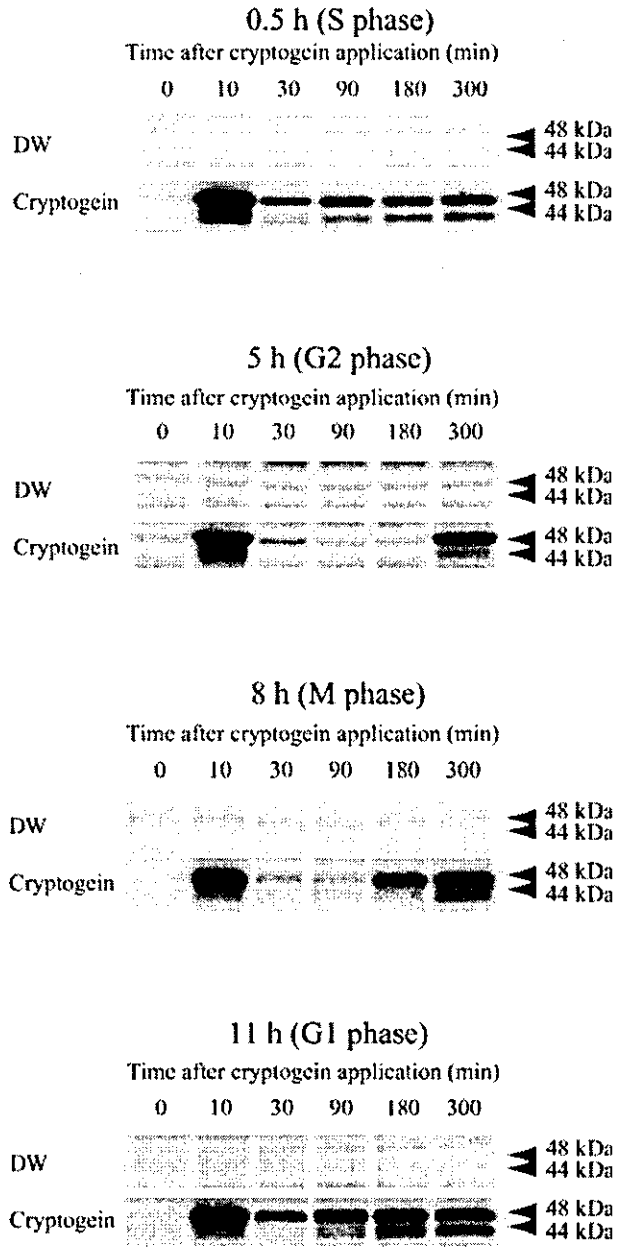

Fig. 2 The cryptogein-induced prolonged activation of MAPKs depends on the phase of the cell cycle. Cryptogein or distilled water (DW) was applied to BY-2 cells at 0.5 h (S phase), 5 h (G_2 phase), 8 h (M phase) or 11 h (G_1 phase) after aphidicolin release. Activation of MAPKs was monitored with an in-gel kinase assay. Experimental conditions were as in Fig. 1. One representative experiment of three independent experiments is shown in each case. A similar cell cycle progression to that shown in Fig. 1 was confirmed by flow cytometric analysis and mitotic index analysis (data not shown).

The slow and prolonged production of ROS depends on the phase of the cell cycle during which cryptogein recognition occurs

To examine cell cycle dependence of the elicitor-induced production of reactive oxygen species, the cryptogein-induced increase in superoxide anion ($^{\cdot}O_2^-$) was monitored during each phase of the cell cycle with chemiluminescence assays using 2-methyl-6-[*p*-methoxyphenyl]-3,7-dihydroimidazo[1,2-α]pyrazin-3-one (MCLA) (Uehara et al. 1993). Treatment with cryptogein at the S or G_1 phases induced $^{\cdot}O_2^-$ production in a bipha-

sic manner, namely a rapid and transient increase that peaked at around 10 min, followed by a slow and prolonged production of $^{\cdot}O_2^-$ that continued for at least 5.5 h (Fig. 3). In contrast, treatment with the elicitor during the G_2 or M phases induced rapid and transient $^{\cdot}O_2^-$ production at 10 min, but the induction of the slow and prolonged $^{\cdot}O_2^-$ production was delayed. Treatment with cryptogein during the G_2 phase resulted in prolonged $^{\cdot}O_2^-$ production at 5.5 h after treatment (10.5 h after aphidicolin release), and treatment during the M phase induced the prolonged $^{\cdot}O_2^-$ production at 3 h after cryptogein application (11 h after aphidicolin release). Since the cells enter the G_1 phase at around 10 h after aphidicolin release (Fig. 1A, B), the induction of the prolonged $^{\cdot}O_2^-$ production corresponds well to the progression of the cell cycle to the G_1 phase. Overall, the rapid and transient production of ROS occurred after cryptogein recognition during any of the phases of the cell cycle, but the slow and prolonged production occurred at S or G_1 phase.

Cryptogein recognition during the G_1 phase, but not the G_2 or M phases, induces cell cycle arrest, the prolonged activation of MAPKs, the prolonged production of ROS, induction of defense-related genes and cell death

The prolonged activation of MAPKs and the prolonged production of ROS did not occur when cryptogein was applied before the progression of the cell cycle to the G_1 phase (Fig. 2, 3). Two hypotheses could explain the cell cycle-dependent activation of these responses. First, recognition of cryptogein during any phase of the cell cycle is sufficient to induce the biphasic activation of MAPKs and the biphasic production of ROS, but the prolonged activation of MAPKs and the prolonged production of ROS are induced only after cell cycle progression to G_1 phase. Alternatively, recognition of cryptogein during the S or G_1 phases is required to induce the prolonged activation of MAPKs and the prolonged production of ROS. To determine whether the recognition of cryptogein at the G_1 phase is prerequisite to induce the prolonged activation of MAPKs and the prolonged production of ROS, cryptogein was applied to cells in the G_2 phase (5 h after aphidicolin release) and removed before the cells progressed to the G_1 phase (9 h after aphidicolin release) by extensive washing with growth medium (Fig. 4A). When cryptogein was removed before the G_1 phase, the cryptogein-induced prolonged activation of MAPKs (Fig. 4B) and prolonged production of ROS

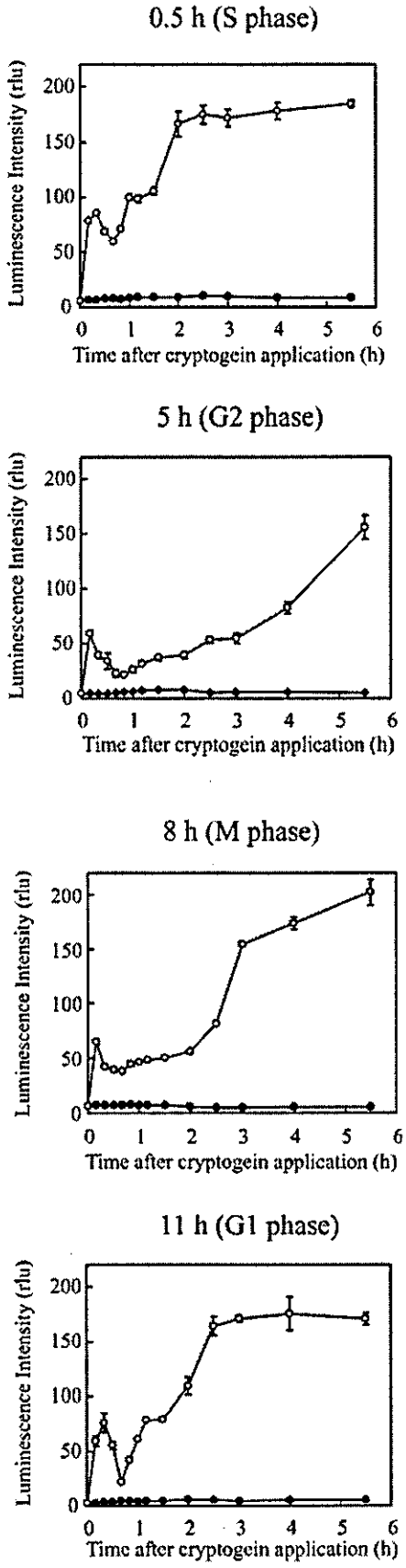

Fig. 3 Cryptogein-induced prolonged production of $^{\cdot}O_2^-$ depends on the phase of the cell cycle. Cryptogein (open circles) or distilled water (solid circles) was applied to BY-2 cells at 0.5 h (S phase), 5 h (G_2 phase), 8 h (M phase) or 11 h (G_1 phase) after aphidicolin release. Production of $^{\cdot}O_2^-$ was monitored with chemiluminescence assays using MCLA. The luminescence intensity, which reflects the $^{\cdot}O_2^-$ concentration, was monitored with a luminometer. Experimental conditions were as in Fig. 1. One representative experiment of three independent experiments is shown in each case. A similar cell cycle progression to that shown in Fig. 1 was confirmed by flow cytometric analysis and mitotic index analysis (data not shown).

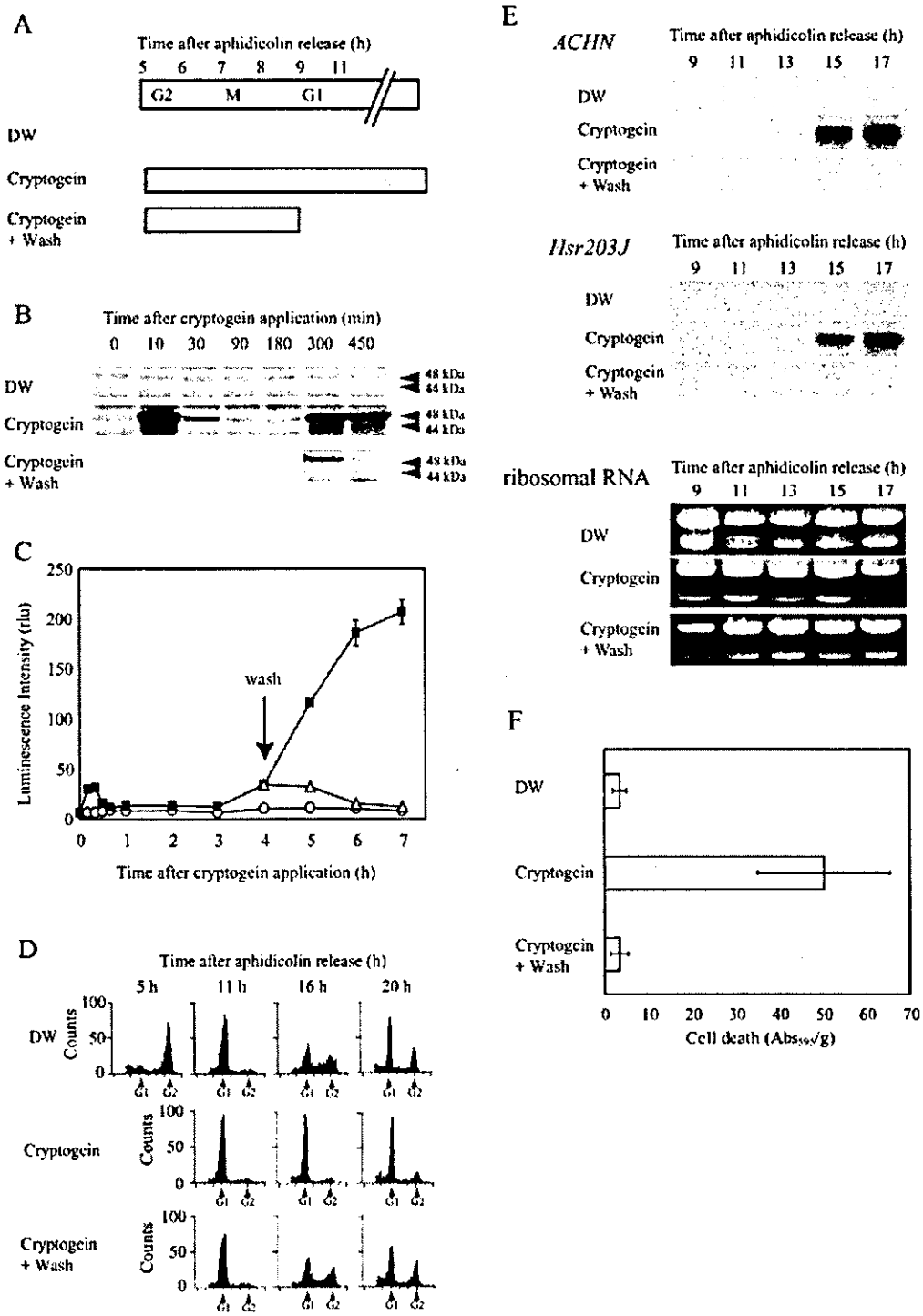

(Fig. 4C) did not occur, suggesting that the recognition of cryptogein during the G_1 phase is necessary to induce these responses. Similar results were obtained for the following downstream events, including cell cycle arrest (Fig. 4D), accumulation of defense-related gene transcripts (Fig. 4E) and cell death (Fig. 4F).

Flow cytometric analysis showed that cells treated with distilled water progressed from the S phase to the G_2 phase (5 h after aphidicolin release) and subsequently to the G_1 (11 h) and G_2 phases (16 and 21 h), whereas continuous treatment with cryptogein induced G_1 phase arrest. When cryptogein was removed before the cells progressed to the G_1 phase, the cells

did not induce G_1 phase arrest but, instead, progressed normally to the G_2 phase (16 and 21 h). These results suggest that the recognition of cryptogein at the G_1 phase, but not at the G_2 or M phases, induces cell cycle arrest.

The amounts of transcripts of the defense-related genes *Hsr203j* and *ACHN* (acidic chitinase) were analyzed using RNA gel blot analysis. *Hsr203j*, a hypersensitive response-related (*hsr*) gene encoding a serine hydrolase with esterase activity (Baudouin et al. 1997), has been postulated as regulating either the establishment or the limitation of cell death (Pontier et al. 1998), and *ACHN* encodes a chitinase that breaks down the cell walls of microbes (Linthorst et al. 1990). Continuous treatment with cryptogein induced the accumulation of transcripts of these genes, but removal of the elicitor before the G_1 phase inhibited the accumulation.

Continuous treatment with cryptogein induced cell death, as detected using the Evans blue assay, but removal of the elicitor before the G_1 phase led to inhibition of the elicitor-induced cell death. Therefore, recognition of cryptogein at the G_1 phase, but not at the G_2 or M phases, induces the prolonged activation of MAPKs, the prolonged production of ROS, cell cycle arrest, the accumulation of transcripts of defense-related genes and cell death.

Discussion

One of the signaling components altered by the cell cycle phases acts between the perception of the cryptogein elicitor signal and the influx of Ca^{2+} through the plasma membrane

The change in the $[Ca^{2+}]_{cyt}$ is one of the earliest responses induced by treatment with elicitors. After an apparent lag of around 1 min, cryptogein induced two characteristic transient increases in the $[Ca^{2+}]_{cyt}$ (Kadota et al. 2004a). Pharmacological experiments have shown that the first peak of the biphasic increase in $[Ca^{2+}]_{cyt}$ corresponds to the influx of Ca^{2+} through the plasma membrane; this influx may activate the second peak in the $[Ca^{2+}]_{cyt}$ increase that results from the release of Ca^{2+} from the intracellular Ca^{2+} stores via an inositol triphosphate-dependent pathway. Although no clear biphasic changes in the $[Ca^{2+}]_{cyt}$ could be detected in the synchronized cultured cells, possibly because of overlap of the two peaks, cryptogein-induced $[Ca^{2+}]_{cyt}$ changes clearly occurred at all phases of the cell cycle, suggesting that cryptogein recognition occurred at all cell cycle phases. Given that the aequorin luminescence of the first peak in the $[Ca^{2+}]_{cyt}$ is 2- to 3-fold greater than that of the second peak (Kadota et al. 2004a), the significantly weaker cryptogein-induced $[Ca^{2+}]_{cyt}$ increase during the G_2 and M phases (Fig. 1C) indicates that the cryptogein-induced plasma membrane Ca^{2+} influx (the first peak in the $[Ca^{2+}]_{cyt}$) is at least partially suppressed in the G_2 and M phases. These results suggest that one of the signaling component(s) that vary during the different phases of the cell cycle is active between the time of perception of the elicitor signal and the influx of Ca^{2+} through the plasma membrane. Although the cryptogein receptor has not yet been identified, the receptor may be one of the strong candidates for the signaling component differently regulated during cell cycle phases. Microarray analysis of a synchronized suspension of the *Arabidopsis* cell culture MM2d showed that transcripts of two putative disease resistance proteins (accession numbers At4g36140 and At2g24160) accumulate during the G_1 and S phases (Menges et al. 2002). This result might support the hypothesis that the cryptogein receptor is partially inactivated during the G_2 or M phases.

Future analysis on the expression of the receptors of elicitors and disease resistance genes, as well as the activity of these products during each phase of the cell cycle, may lead to a better understanding of the cell cycle dependence of elicitor signaling in plants.

The patterns of the cryptogein-induced production of ROS and activation of MAPKs differ drastically in different phases of the cell cycle

Although ROS production and activation of MAPKs triggered by cell death-inducing elicitors have been reported in various systems, the characteristics of these responses differ, and have been controversial. Pugin et al. (1997) and Simon-Plas et al. (2002) showed that cryptogein induces a transient production of ROS in a tobacco cell suspension, with a single peak at 30 min. In contrast, hypersensitive response-inducing pathogens or elicitors induce two peaks in the generation of ROS in other systems (Chandra et al. 1996, Lamb and Dixon 1997, Grant and Loake 2000, Yoshioka et al. 2001).

Fig. 4 Cell cycle arrest, the prolonged activation of MAPKs, the prolonged production of $^{\cdot}O_2^-$, the expression of defense-related genes and cell death were induced after cryptogein treatment during the G_1 phase. (A) Cryptogein or distilled water (DW) was applied to BY-2 cells at 5 h (G_2 phase) after aphidicolin release, and then the cryptogein was removed by extensive washing with growth medium at 9 h (M/G_1). All experiments in this figure were performed with these conditions. (B) Activation of MAPKs was monitored with an in-gel kinase assay. One experiment representative of three independent experiments is shown in each case. (C) Production of $^{\cdot}O_2^-$ was monitored by the MCLA chemiluminescence. Cryptogein (solid squares) or DW (open circles) was applied to BY-2 cells at 5 h (G_2 phase) after aphidicolin release, and then the cryptogein was removed by extensive washing with growth medium at 9 h (M/G1, open triangles). One experiment, representative of three independent experiments, is shown in each case. (D) The effect of cryptogein on the progression of the cell cycle in BY-2 cells. The cell cycle progression was monitored by flow cytometric analysis. One experiment, representative of three independent experiments, is shown in each case. (E) RNA gel blot analysis of the defense-related genes *ACHN* and *Hsr203J*. One experiment, representative of three independent experiments, is shown in each case. (F) Induction of cell death at 40 h after aphidicolin release was detected using the Evans blue assay. A similar cell cycle progression to that shown in Fig. 1 was confirmed by flow cytometric and mitotic index analyses (data not shown). Representative results of three independent experiments are shown.

Lebrun-Garcia et al. (1998) showed that cryptogein induces a transient activation of SIPK- and WIPK-like protein kinases that peaks at 30 min post-treatment and gradually decreases to the basal level. Romeis et al. (1999) also showed that the avirulence gene product Avr9 induces a transient activation of SIPK- and WIPK-like protein kinases that peaks at 15 min post-treatment in tobacco suspension cultures expressing the resistance gene product Cf9. In contrast, Zhang et al. (1998) showed that cryptogein induces the prolonged activation of a SIPK-like protein kinase that continues for at least 8 h. Likewise, Suzuki et al. (1999) showed that treatment with xylanase induces the prolonged activation of a SIPK-like protein kinase that is sustained for at least 4 h, after which the activity decreases to the basal level within 2 h. We have shown in the present study that the patterns of the cryptogein-induced production of ROS and the activation of both MAPKs change drastically, depending on the phase of the cell cycle (Fig. 2, 3). These results may give us a clue that explains why the characteristics of the ROS production and activation of MAPKs triggered by cell death-inducing elicitors are sometimes different in different systems. The patterns of these changes may be different between proliferating cells and resting cells, and may also reflect the growth stage. Furthermore, our results may suggest that interpretation of previously reported results regarding the production of ROS and activation of MAPKs during defense responses should be revised, with consideration given to the phase of the cell cycle.

The cryptogein-induced slow and prolonged activation of MAPKs and the slow and prolonged production of ROS are dependent on the phase of the cell cycle

ROS play important roles in the induction of hypersensitive responses in plants (Levine et al. 1994, Lamb and Dixon 1997). In many experimental systems in which biphasic production of ROS is induced upon elicitation, the rapid and transient production of ROS (phase I), which occurs within minutes of the perception of pathogens, is not specific to hypersensitive responses, because compatible pathogens that do not induce hypersensitive responses also elicit this peak. In contrast, the second phase of ROS production (phase II) is specific to infection with hypersensitive response-inducing pathogens (Chandra et al. 1996, Lamb and Dixon 1997, Grant and Loake 2000, Yoshioka et al. 2001). We here showed that the rapid and transient production of ROS (phase I) occurred after elicitation, during any phase of the cell cycle, whereas the second increase in ROS (phase II) occurred only after elicitation during the S or G_1 phases (Fig. 3). The second increase in ROS production (phase II) in the S and G_1 phases correlates well with the cryptogein-induced accumulation of transcripts of defense-related genes and cell death, which are only induced by treatment with cryptogein during the S or G_1 phases (Kadota et al. 2004b).

The prolonged activation of MAPKs is correlated with defense responses and is thought to be important for the induction of cell death and defense-related gene expression (Suzuki et al. 1999, Ren et al. 2002). We have demonstrated that the prolonged activation of MAPKs occurs only after elicitation during the G_1 and S phases, whereas the rapid and transient activation of MAPKs can occur after elicitation during any of the phases of the cell cycle (Fig. 2). The prolonged activation of MAPKs is also strongly correlated with the induction of cell death. Suppression of defense responses in G_2 or M phases may be attributed to the absence of prolonged production of ROS and prolonged activation of MAPKs. Alternatively, it might also be possible that many other components that participate in induction of defense responses are inactivated during G_2 or M phase.

Relationships among the cryptogein-induced signaling events, including the increase in $[Ca^{2+}]_{cyt}$, the activation of MAPKs, and ROS production

The elicitor-induced expression of the *Rboh* (respiratory burst oxidase homolog) gene is thought to contribute to the slow and prolonged production of ROS, following the rapid and transient production (Yoshioka et al. 2001). The overexpression of MEK^{DD}, a constitutively active mutant of a MAPK kinase, induces the activation of SIPK and WIPK, the expression of the *Nicotiana benthamiana Rboh* homolog *NbRbohB*, and hypersensitive-like cell death (Yang et al. 2001, Yoshioka et al. 2003), suggesting that a MAPK cascade positively regulates ROS production. Absence of the prolonged activation of MAPKs by cryptogein application in the G_2 and M phases may result in the inhibition of the slow and prolonged production of ROS and cell death.

The inhibition of the cryptogein-induced increase in $[Ca^{2+}]_{cyt}$ during the G_2 and M phases correlates well with the absence of the prolonged production of ROS and the prolonged activation of MAPKs during these phases (Fig. 1C, 2, 3). Multiple reports have indicated that Ca^{2+} chelators and Ca^{2+} channel blockers completely inhibit elicitor-induced ROS production and activation of MAPKs, suggesting that the Ca^{2+} influx is essential for the induction of these responses (Suzuki and Shinshi 1995, Tavernier et al. 1995, Romeis et al. 1999, Suzuki et al. 1999, Lecourieux et al. 2002, Kadota et al. 2004a). However, whether the inhibition of the cryptogein-induced increase in $[Ca^{2+}]_{cyt}$ in the G_2 and M phases is responsible for the absence of the prolonged production of ROS, and the prolonged activation of MAPKs, is still unclear. Interestingly, treatment with cryptogein during the G_2 and M phases induces rapid and transient ROS production and rapid and transient activation of MAPKs, but changes in the $[Ca^{2+}]_{cyt}$ were suppressed during these phases. This suggests that a slight increase in $[Ca^{2+}]_{cyt}$ during the G_2 and M phases is sufficient to induce the rapid and transient ROS production, and the rapid and transient activation of MAPKs. These results suggest that the transient MAPK activation and ROS production occur independently of the prolonged version of both phenomena.

Defense responses are not induced during the G_2 and M phases

Treatment with cryptogein during the G_2 or M phases did not induce the prolonged activation of MAPKs (Fig. 4B), the prolonged production of ROS (Fig. 4C), cell cycle arrest (Fig. 4D), the expression of two defense-related genes (Fig. 4E) or cell death (Fig. 4F); however, treatment with cryptogein during the S or G_1 phases did induce these responses (Fig. 2, 3; Kadota et al. 2004b). Since treatment with cryptogein during G_2 and M phases induced the rapid and transient production of ROS and the rapid and transient activation of MAPKs, cells in these phases are not insensitive to cryptogein but are not able to induce downstream events including prolonged activation of MAPK, prolonged production of ROS, expression of defense-related genes and cell death.

Cells treated continuously with cryptogein during the G_2 or M phases showed prolonged activation of MAPKs and prolonged production of ROS after progression to the G_1 phase (Fig. 2, 3). Are the rapid and transient activation of MAPKs and the rapid and transient production of ROS induced again in the G_1 phase? It was exceedingly difficult to detect these responses in the G_1 phase because of the short duration of these responses. Transient treatment of the cells with cryptogein during the G_2 phase (5–7 h), and again at the G_1 phase (11 h), induced the transient activation of MAPKs and transient production of ROS at the G_2 phase, as well as biphasic activation of MAPKs and biphasic production of ROS at the G_1 phase, with characteristics similar to those induced by cryptogein treatment only during the G_1 phase (data not shown). These results suggest that the rapid and transient activation of MAPKs, and the rapid and transient production of ROS, are induced again in the G_1 phase.

In conclusion, we have demonstrated that cryptogein signaling events, including the increase in $[Ca^{2+}]_{cyt}$, ROS production, activation of MAPKs, expression of defense-related genes and cell death, are regulated in a cell cycle-dependent manner. Further studies using this model system should allow a better understanding of the cell cycle dependence of defense signaling at the molecular level.

Materials and Methods

Plant material

The tobacco BY-2 (*Nicotiana tabacum* L. cv. Bright Yellow 2) suspension was maintained by weekly dilution (1/100) of cells in modified Linsmaier and Skoog (LS) medium, as described by Nagata et al. (1992). The cell suspension was agitated on a rotary shaker at 100 rpm at 28°C in the dark.

Expression and purification of cryptogein

Pichia pastoris (strain GS115) bearing the plasmid pLEP3 was used to produce cryptogein. Cryptogein was expressed according to O'Donohue et al. (1996) and was dissolved in distilled water. The cryptogein concentration was determined using UV spectroscopy with an extinction coefficient of 8,306 M^{-1} cm^{-1} at 277 nm (O'Donohue et al. 1995).

Cell cycle synchronization

A stationary culture of tobacco BY-2 cells was diluted 1/10 in fresh modified LS medium supplemented with 5 μg/ml aphidicolin (Wako Pure Chemical, Japan). After 24 h of culture, the aphidicolin was removed by extensive washing and the cells were resuspended in fresh medium.

Determination of the cell division percentages of the BY-2 cells

The cell division percentages were obtained by determining the mitotic index after staining of the cells with 4',6-diamidino-2-phenylindole (DAPI) and observation under a fluorescence microscope.

Flow cytometric analysis

Flow cytometric analysis was performed according to the manufacturer's protocol as follows. A 1 ml aliquot of cell suspension was centrifuged at 1,000×*g* for 1 min. Approximately 500 μl of Nuclear Isolation and Staining Solution 3 (NPE Systems, Inc. Pembroke Pines, FL, U.S.A.) were added to the cell suspension pellet. The cells were chopped with a razor blade and then incubated for 10 min at room temperature, after which the nuclei were separated from the cells by filtering the mixture through a 100 μm nylon filter. The fluorescence intensity was measured by flow cytometry [NPE Quanta(TM), NPE Systems, Inc.]. Counts with low fluorescence intensity contained fluorescence from DNA fragmented during the extraction of the nuclei. Therefore, counts were disregarded below a cut-off value of a much lower fluorescence intensity than that of nuclei at the G_1 phase.

Measurement of changes in the $[Ca^{2+}]_{cyt}$

The apoaequorin-expressing BY-2 cell suspension was incubated with 1 μM coelenterazine for at least 6 h. The aequorin luminescence, which reflects the $[Ca^{2+}]_{cyt}$, was measured with a Lumicounter 2500 luminometer (Microtech Nition, Funabashi, Japan) equipped with an A/D converter (MacLab, AD instruments, Castle Hill, Australia), and data were analyzed using the program Chart v. 3.6.8 (AD Instruments). Cell samples of 250 μl were transferred to cylindrical plastic cuvettes and held for 15 min at room temperature, with stirring at 150 rpm to allow the cells to recover from the mechanical stress caused by pipetting. Cuvettes containing the cell suspension were placed in the luminometer and rotated 17 times every 3 s, alternatively clockwise and counterclockwise, to stir the cells during luminescence measurement. The total luminescence intensities after the addition of a 20% volume of 1 M $CaCl_2$/20% ethanol solution were analyzed in each phase of the cell cycle, and the cryptogein-induced aequorin luminescence curves were normalized with the total luminescence of the same sample, so that the values of aequorin luminescence in each phase of the cell cycle can be compared with each other.

In-gel kinase assay

Extracts containing 20 μg of protein were electrophoresed on 10% SDS–polyacrylamide gels embedded with 0.25 mg ml^{-1} of myelin basic protein (MBP) in the separating gel as a substrate for the kinase. Following electrophoresis, the SDS was removed by washing the gels three times for 30 min with washing buffer [25 mM Tris, pH 7.5, 0.5 mM dithiothreitol (DTT), 0.1 mM Na_3VO_4, 5 mM NaF, 0.5 mg ml^{-1} bovine serum albumin (BSA), 0.1% Triton X-100 (v/v)] at room temperature. The kinases were allowed to renature overnight in 25 mM Tris, pH 7.5, 1 mM DTT, 0.1 mM Na_3VO_4 and 5 mM NaF at 4°C with three changes of buffer. The gels were then incubated at room temperature for 60 min in 30 ml of reaction buffer (25 mM Tris, pH 7.5, 2 mM EGTA, 12 mM $MgCl_2$, 1 mM DTT, 0.1 mM Na_3VO_4) containing 200 nM ATP and 50 μCi of [γ-^{32}P]ATP (3,000 Ci $mmol^{-1}$). The reaction was stopped by transferring the gels into 5% trichloroacetic acid (TCA) (w/v)/1% NaPPi (w/v). The unincorporated [γ-^{32}P]ATP

was removed by washing in the same solution for at least 6 h with five changes. The gels were dried onto Whatman 3 MM paper and exposed to imaging plates (Fuji Film Co., ltd, Tokyo, Japan). Signals were visualized with Typhoon 9210 (Amersham-Pharmacia Biotech).

Measurement of $^{\cdot}O_2^-$ production

BY-2 cell suspensions were washed and resuspended in fresh growth medium 30 min before measurement. A 250 µl aliquot of cell suspension was sampled at the indicated time and treated with 2 µM MCLA (Molecular Probes, Eugene, OR, U.S.A.); the $^{\cdot}O_2^-$-dependent luminescence was measured with a Lumicounter 2500 (Microtech Nition, Chiba, Japan).

RNA extraction and Northern analysis

Total RNA was extracted from each frozen cell sample using TRIzol reagent, according to the manufacturer's instructions (Invitrogen Co., Carlsbad, CA, U.S.A.). Denatured total RNA (15 µg) was electrophoresed in 2% agarose gels containing 5.5% formaldehyde and transferred to Hybond-N membrane (Amersham-Pharmacia Biotech, Little Chalfont, U.K.). Hybridization was performed at 65°C in phosphate buffer (500 mM Na-phosphate, pH 7.2, 1 mM EDTA, 1% BSA, 7% SDS) with random-primed ^{32}P-labeled probes prepared from tobacco cDNAs corresponding to the *ACHN* (Linthorst et al. 1990) and *Hsr203J* (Baudouin et al. 1997) genes. Hybridization signals were visualized with a Bioimage Analyzer (BAS-2000, Fuji Film, Japan) and Typhoon 9210 (Amersham-Pharmacia Biotech).

Cell death assay

A 1 ml aliquot of the cell suspension was incubated with 0.05% Evans blue (Sigma, St. Louis, MO, U.S.A.) for 15 min and then washed to remove unabsorbed dye. The selective staining of dead cells with Evans blue depends on the extrusion of the dye from living cells via the intact plasma membrane. The dye passes through the damaged membranes of dead cells and accumulates as a blue protoplasmic stain (Turner and Novacky 1974). Dye that had been absorbed by dead cells was extracted in 50% methanol/1% SDS for 1 h at 60°C and quantified by absorbance at 595 nm.

Acknowledgments

The authors thank Dr. Kaoru Suzuki for generous gifts of cDNA clones for *ACHN* and *Hsr203J* and for helpful discussions, Professor Jean-Claude Pernollet for providing us with the cryptogein gene, Drs. Masaaki Umeda and Toyoki Amano for valuable suggestions, Mr. Toshikazu Yagala for technical assistance, and Mr. Takumi Higaki for critical reading of the manuscript. This work was supported in part by a Grant-in-Aid for the Research for the Future Program and Scientific Research (B) (No. 14340251), from the Japan Society for the Promotion of Science, to K.K. and by Grants-in-Aid for Scientific Research in Priority Areas from the Ministry of Education, Science, Culture, Sports, and Technology, Japan, to K.K. (No. 13039015).

References

Asai, T., Tena, G., Plotnikova, J., Willmann, M.R., Chiu, W.L., Gómez-Gómez, L., Boller, T., Ausubel, F.M. and Sheen, J. (2002) MAP kinase signalling cascade in *Arabidopsis* innate immunity. *Nature* 415: 977–983.

Baudouin, E., Charpenteau, M., Roby, D., Marco, Y., Ranjeva, R. and Ranty, B. (1997) Functional expression of a tobacco gene related to the serine hydrolase family—esterase activity towards short-chain dinitrophenyl acylesters. *Eur. J. Biochem.* 248: 700–706.

Chandra, S., Martin, G.B. and Low, P.S. (1996) The Pto kinase mediates a signaling pathway leading to the oxidative burst in tomato. *Proc. Natl Acad. Sci. USA* 93: 13393–13397.

Grant, J.J. and Loake, G.J. (2000) Role of reactive oxygen intermediates and cognate redox signaling in disease resistance. *Plant Physiol.* 124: 21–29.

Heath, M.C. (2000) Hypersensitive response-related death. *Plant Mol. Biol.* 44: 321–334.

Jones, A.M. and Dangl, J.L. (1996) Logjam at the Styx: programmed cell death in plants. *Trends Plant Sci.* 1: 114–119.

Kadota, Y., Furuichi, T., Ogasawara, Y., Goh, T., Higashi, K., Muto, S. and Kuchitsu, K. (2004c) Identification of putative voltage-dependent Ca^{2+}-permeable channels involved in cryptogein-induced Ca^{2+} transients and defense responses in tobacco BY-2 cells. *Biochem. Biophys. Res. Commun.* 317: 823–830.

Kadota, Y., Goh, T., Tomatsu, H., Tamauchi, R., Higashi, K., Muto, S. and Kuchitsu, K. (2004a) Cryptogein-induced initial events in tobacco BY-2 cells: pharmacological characterization of molecular relationship among cytosolic Ca^{2+} transients, anion efflux and production of reactive oxygen species. *Plant Cell Physiol.* 45: 160–170.

Kadota, Y., Watanabe, T., Fujii, S., Higashi, K., Sano, T., Nagata, T., Hasezawa, S. and Kuchitsu, K. (2004b) Crosstalk between elicitor-induced cell death and cell cycle regulation in tobacco BY-2 cells. *Plant J.* 40: 131–142.

Lamb, C. and Dixon, R.A. (1997) The oxidative burst in plant disease resistance. *Annu. Rev. Plant Physiol. Plant Mol. Biol.* 48: 251–275.

Lebrun-Garcia, A., Ouaked, F., Chiltz, A. and Pugin, A. (1998) Activation of MAPK homologues by elicitors in tobacco cells. *Plant J.* 15: 773–781.

Lecourieux, D., Mazars, C., Pauly, N., Ranjeva, R. and Pugin, A. (2002) Analysis and effects of cytosolic free calcium increases in response to elicitors in *Nicotiana plumbaginifolia* cells. *Plant Cell* 14: 2627–2641.

Levine, A., Tenhaken, R., Dixon, R. and Lamb, C. (1994) H_2O_2 from the oxidative burst orchestrates the plant hypersensitive disease resistance response. *Cell* 79: 583–593.

Linthorst, H.J., van Loon, L.C., van Rossum, C.M., Mayer, A., Bol, J.F., van Roekel, J.S., Meulenhoff, E.J. and Cornelissen, B.J. (1990) Analysis of acidic and basic chitinases from tobacco and petunia and their constitutive expression in transgenic tobacco. *Mol. Plant Microbe Interact.* 3: 252–258.

Logemann, E., Wu, S.C., Schröder, J., Schmelzer, E., Somssich, I.E. and Hahlbrock, K. (1995) Gene activation by UV light, fungal elicitor or fungal infection in *Petroselinum crispum* is correlated with repression of cell cycle-related genes. *Plant J.* 8: 865–876.

Menges, M., Hennig, L., Gruissem, W. and Murray, J.A. (2002) Cell cycle-regulated gene expression in *Arabidopsis*. *J. Biol. Chem.* 277: 41987–42002.

Nagata, T., Nemoto, Y. and Hasezawa, S. (1992) Tobacco BY-2 cell line as the 'Hela' cell in the cell biology of higher plants. *Int. Rev. Cytol.* 132: 1–30.

Nürnberger, T. and Scheel, D. (2001) Signal transmission in the plant immune response. *Trends Plant Sci.* 6: 372–379.

O'Donohue, M.J., Boissy, G., Huet, J.C., Nespoulous, C., Brunie, S. and Pernollet, J.C. (1996) Overexpression in *Pichia pastoris* and crystallization of an elicitor protein secreted by the phytopathogenic fungus, *Phytophthora cryptogea*. *Protein Expr. Purif.* 8: 254–261.

O'Donohue, M.J., Gousseau, H., Huet, J.C., Tepfer, D. and Pernollet, J.C. (1995) Chemical synthesis, expression and mutagenesis of a gene encoding beta-cryptogein, an elicitin produced by *Phytophthora cryptogea*. *Plant Mol. Biol.* 27: 577–586.

Pontier, D., Tronchet, M., Rogowsky, P., Lam, E. and Roby, D. (1998) Activation of hsr203, a plant gene expressed during incompatible plant–pathogen interactions, is correlated with programmed cell death. *Mol. Plant Microbe Interact.* 11: 544–554.

Pugin, A., Frachisse, J.M., Tavernier, E., Bligny, R., Gout, E., Douce, R. and Guern, J. (1997) Early events induced by the elicitor cryptogein in tobacco cells: involvement of a plasma membrane NADPH oxidase and activation of glycolysis and the pentose phosphate pathway. *Plant Cell* 9: 2077–2091.

Ren, D., Yang, H. and Zhang, S. (2002) Cell death mediated by MAPK is associated with hydrogen peroxide production in *Arabidopsis*. *J. Biol. Chem.* 277: 559–565.

Romeis, T., Piedras, P., Zhang, S., Klessig, D.F., Hirt, H. and Jones, J.D. (1999) Rapid Avr9- and Cf-9-dependent activation of MAP kinases in tobacco cell cultures and leaves: convergence of resistance gene, elicitor, wound, and salicylate responses. *Plant Cell* 11: 273–287.

Seo, S., Okamoto, M., Seto, H., Ishizuka, K., Sano, H. and Ohashi, Y. (1995) Tobacco MAP kinase: a possible mediator in wound signal transduction pathways. *Science* 270: 1988–1992.

Simon-Plas, F., Elmayan, T. and Blein, J.P. (2002) The plasma membrane oxidase NtrbohD is responsible for AOS production in elicited tobacco cells. *Plant J.* 31: 137–147.

Suzuki, K. and Shinshi, H. (1995) Transient activation and tyrosine phosphorylation of a protein kinase in tobacco cells treated with a fungal elicitor. *Plant Cell* 7: 639–647.

Suzuki, K., Yano, A. and Shinshi, H. (1999) Slow and prolonged activation of the p47 protein kinase during hypersensitive cell death in a culture of tobacco cells. *Plant Physiol.* 119: 1465–1472.

Takahashi, K., Isobe, M., Knight, M.R., Trewavas, A.J. and Muto, S. (1997) Hypoosmotic shock induces increases in cytosolic Ca^{2+} in tobacco suspension-culture cells. *Plant Physiol.* 113: 587–594.

Tavernier, E., Wendehenne, D., Blein, J.P. and Pugin, A. (1995) Involvement of free calcium in action of cryptogein, a proteinaceous elicitor of hypersensitive reaction in tobacco cells. *Plant Physiol.* 109: 1025–1031.

Turner, J.G. and Novacky, A. (1974) The quantitative relation between plant and bacterial cells involved in the hypersensitive reaction. *Phytopathology* 64: 885–890.

Uehara, K., Maruyama, N., Huang, C.K. and Nakano, M. (1993) The first application of a chemiluminescence probe, 2-methyl-6-[*p*-methoxyphenyl]-3, 7-dihydroimidazo[1, 2-α]pyrazin-3-one (MCLA), for detecting O_2^- production, in vitro, from Kupffer cells stimulated by phorbol myristate acetate. *FEBS Lett.* 335: 167–170.

Yang, K.Y., Liu, Y. and Zhang, S. (2001) Activation of a mitogen-activated protein kinase pathway is involved in disease resistance in tobacco. *Proc. Natl Acad. Sci. USA* 98: 741–746.

Yoshioka, H., Sugie, K., Park, H.J., Maeda, H., Tsuda, N., Kawakita, K. and Doke, N. (2001) Induction of plant gp91 phox homolog by fungal cell wall, arachidonic acid, and salicylic acid in potato. *Mol. Plant Microbe Interact.* 14: 725–736.

Yoshioka, H., Numata, N., Nakajima, K., Katou, S., Kawakita, K., Rowland, O., Jones, J.D. and Doke, N. (2003) *Nicotiana benthamiana* gp91phox homologs NbrbohA and NbrbohB participate in H_2O_2 accumulation and resistance to *Phytophthora infestans*. *Plant Cell* 15: 706–718.

Zhang, S., Du, H. and Klessig, D.F. (1998) Activation of the tobacco SIP kinase by both a cell wall-derived carbohydrate elicitor and purified proteinaceous elicitins from *Phytophthora* spp. *Plant Cell* 10: 435–450.

Zhang, S. and Klessig, D.F. (2000) Pathogen-induced MAP kinases in tobacco. *Results Probl. Cell Differ.* 27: 65–84.

(Received August 21, 2004; Accepted October 27, 2004)

Plant Cell Physiol. 45(10): 1371–1379 (2004)
JSPP © 2004

Three Types of Tobacco Calmodulins Characteristically Activate Plant NAD Kinase at Different Ca^{2+} Concentrations and pHs

Eri Karita [1,2,3,5], Hiromoto Yamakawa [2,3,5,6], Ichiro Mitsuhara [2,3], Kazuyuki Kuchitsu [1,4] and Yuko Ohashi [2,3,7]

[1] *Department of Applied Biological Science, Tokyo University of Science, 2641 Yamazaki, Noda, Chiba, 278-8510 Japan*
[2] *Plant Physiology Department, National Institute of Agrobiological Sciences, Tsukuba, Ibaraki, 305-8602 Japan*
[3] *PROBRAIN, Japan Science and Technology Corporation, Chiyoda-ku, Tokyo, 101-0062 Japan*
[4] *Genome and Drug Research Center, Tokyo University of Science, 2641 Yamazaki, Noda, Chiba, 278-8510 Japan*

We previously reported that three types of tobacco calmodulin (CaM) isoforms originated from 13 genes are differently regulated at the transcript and protein levels in response to wounding and tobacco mosaic virus-induced hypersensitive reaction (HR); wound-inducible type I and HR-inducible type III levels increased after wounding and HR, respectively, while type II, whose expression is constitutive and wound responsible, remained unchanged. Here, we show that these CaMs differentially activate target enzymes; rat NO synthase was activated most effectively by type III, moderately by type I and weakly by type II, and plant NAD kinase (NADK) was activated in the inverse order. Furthermore, we found that a suitable Ca^{2+} concentration differs by type; type II activated NADK at lower Ca^{2+} of around 0.1 μM, which is the cytosolic concentration in unstimulated cells, type I did so at 1–5 μM, which is the increased Ca^{2+} concentration in stimulated cells, while type III did not at any Ca^{2+} level. NADK activation was highest over a pH range of 7.1–6.8 for which the cytosolic pH reportedly changed from 7.5 after being stimulated. Thus, tobacco CaMs, especially type I, effectively activate NADK in stimuli-induced conditions.

Keywords: Calmodulin — Calcium — NAD kinase — NO synthase — Tobacco.

Abbreviations: CaM, calmodulin; $[Ca^{2+}]_{cyt}$, cytosolic Ca^{2+} concentration; CaN, calcineurin; HR, hypersensitive reaction; NADK, NAD^+ kinase; NO, nitric oxide; NOS, nitric oxide synthase; PR, pathogenesis-related; ROS, reactive oxygen species; TMV, tobacco mosaic virus.

Introduction

We studied the resistance mechanism active against wounding and pathogen infection in plants using wounded and tobacco mosaic virus (TMV)-infected tobacco leaves containing the *N* resistance gene (*Nicotiana tabacum* L. cv Samsun NN). *N* gene-dependent formation of necrotic lesions in virus-infected tissue is a kind of programmed cell death responsible for virus enclosure, and is a hypersensitive reaction (HR) that occurs during the plant's defense response (Goodman and Novacky 1994). It induces both salicylic acid-dependent signaling and jasmonic acid/ethylene-dependent signaling, which mimic wound signaling (Niki et al. 1998). As a HR-responsive gene, we isolated the calmodulin gene (*CaM*), which encodes a major Ca^{2+} receptor that activates target enzymes in the presence of Ca^{2+} (Klee and Vanaman 1982). Although the nature of the downstream signaling of CaM in plant cells is largely unknown, plants have multiple CaM isoforms, which are highly divergent, in contrast to the invariant mammalian CaM (Lee et al. 1995, Takezawa et al. 1995). Therefore, it is expected that multiple plant-specific CaM-mediated signaling pathways exist. Furthermore, a number of studies indicated that the production of reactive oxygen species (ROS) such as O_2^-, H_2O_2 and nitric oxide (NO) plays an important role in the defense response, and is controlled in a Ca^{2+}-dependent manner (Nürnberger et al. 1994, Hahlbrock et al. 1995, Delledonne et al. 1998, Park et al. 1998, Grant et al. 2000).

On the other hand, change in the concentration of cytosolic free Ca^{2+} ($[Ca^{2+}]_{cyt}$) is evoked by various extracellular stimuli including pathogenic infection or elicitors (Sanders et al. 1999, Kadota et al. 2004). Increased $[Ca^{2+}]_{cyt}$ is thought to be required to induce an array of defense responses including ROS production and gene expression via various Ca^{2+} receptors (Reddy 2001). To determine how Ca^{2+} triggers such responses, we successfully isolated 13 *CaM* genes, *NtCaM1-13*, from TMV-infected or wounded tobacco belonging to three plant-specific types (Yamakawa et al. 2001; Fig. 1A). Among them, type I isoforms encoded by *NtCaM1* and *2* showed overall similarities to PCM1, a potato CaM (Takezawa et al. 1995), while type II isoforms, which contain NtCaM3/4/5/6/7/8/9/10/11/12, are highly homologous to soybean SCaM-1. NtCaM13 belongs to type III, and has the most diverse substitutions, which are common to SCaM-4 (Lee et al. 1995). In soybean plant, SCaM-1 and SCaM-4 were characterized by different spectra on activation of target enzyme (Lee et al. 1995, Cho et

[5] These two authors contributed equally to this work.
[6] Present address: National Agricultural Research Center, Joetsu, Nigata, 943-0193 Japan
[7] Corresponding author: E-mail, yohashi@affrc.go.jp; Fax, +81-298-38-7469.

A

```
I    NtCaM 1                1:MAEQLTEEQIAEFKEAFSLFDKDGDGCITTKELGTVMRSLGQNPTEAELQDMISEVDADQ 60
     Potato PCM1            1:.....................................................A..... 60
II   NtCaM 3                1:..D...DD..S.....................................N....G 60
     Soybean SCaM1          1:..D...D...S.....................................N....G 60
     Arabidopsis AtCaM6     1:..D...DD..S.....................................N....G 60
     Arabidopsis AtCaM1     1:..D...D...S.....................................N....G 60
     Potato PCM8            1:..D....D..S.....................................N....G 60
III  NtCaM13                1:.GDI.NQD..V.LQ.....R.....VE..A..I...D.....E.....T..S.G 60
     Soybean SCaM4          1:..DI.S....VD.....G.....VE..A..I...D.....E.....G 60
     Bovine CaM             1:..D.....................T.....................N....G 60

I    NtCaM 1                61:NGTIDFPEFLNLMARKMKDTDSEEELKEAFKVFDKDQNGFISAAELRHVMTNLGEKLTDE 120
     Potato PCM1            61:.....................................................  120
II   NtCaM 3                61:.....................R.....................  120
     Soybean SCaM1          61:.....................R.....................  120
     Arabidopsis AtCaM6     61:.....................R.....................S..  120
     Arabidopsis AtCaM1     61:.....K...............R.....................  120
     Potato PCM8            61:.....................R.....................  120
III  NtCaM13                61:...E.T.....K.....A.....Y..N.....I.....  120
     Soybean SCaM4          61:...E.D...S...K.V....A.....Y...S.....I.....  120
     Bovine CaM             61:.....TM.............IR...R.....G..Y.....  120

I    NtCaM 1                121:EVDEMIREADIDGDGQVNYEEFVRMMLAK- 149
     Potato PCM1            121:.....................- 149
II   NtCaM 3                121:.....V.....I.....KV.M..- 149
     Soybean SCaM1          121:.....V.....I.....KV.M..- 149
     Arabidopsis AtCaM6     121:.....V.....I.....KV.M..- 149
     Arabidopsis AtCaM1     121:..E.....V.....I.....KI.M..- 149
     Potato PCM8            121:.....V.....I..D..KV.M..- 149
III  NtCaM13                121:..EQ..K...L.....FD...K..MNVG 150
     Soybean SCaM4          121:..EQ..K...L.....K..MTVR 150
     Bovine CaM             121:.....Q..T..- 149
```

B

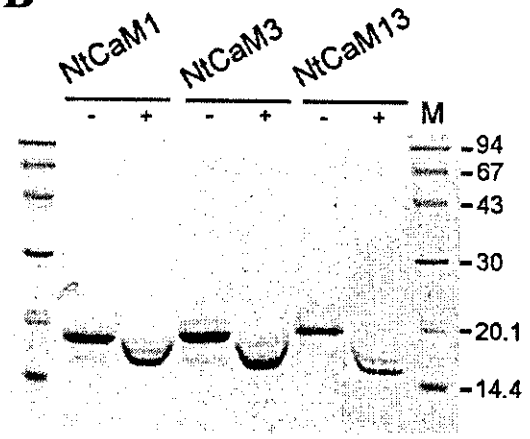

Fig. 1 The characteristics of three types of NtCaMs. (A) Comparison of three plant-specific CaMs and vertebrate CaM amino acid sequences. Dots indicate amino acids identical to those of NtCaM1. Shadows behind the letters indicate four conserved Ca^{2+} binding motifs, EF-hands. (B) Purified NtCaM proteins prepared as described previously (Fromm and Chua 1992). Four micrograms each of recombinant NtCaM1, NtCaM3 and NtCaM13 protein were subjected to 12% SDS–PAGE in the presence of 7.5 mM $CaCl_2$ (+) or 7.5 mM EGTA (–), and protein in the gel was stained with Coomassie Brilliant Blue R-250. The Ca^{2+}/CaM complex migrated more quickly than CaM alone. Molecular weight marks (M) are indicated on the right.

al. 1998), suggesting different functions. Among the three types of plant CaMs, there is little biochemical information on type I CaM except from a gene expression study on potato PCM1 (Takezawa et al. 1995). To characterize the precise functions of each type of CaM, a comparative study was necessary using all CaMs from the same plant source under the same conditions. In this paper, we compared the biochemical nature of type I, II and III CaMs, using purified representative CaMs, NtCaM1, 3 and 13 (Fig. 1B), respectively. For a target enzyme, we selected plant NAD kinase (NADK), which is suggested to function in the self-defense of plants by providing the cofactor NADP for ROS production by NADPH oxidase (Harding et al. 1997). We found that the enzyme was specifically activated by wound-inducible types I and II, whose ratio of total CaMs

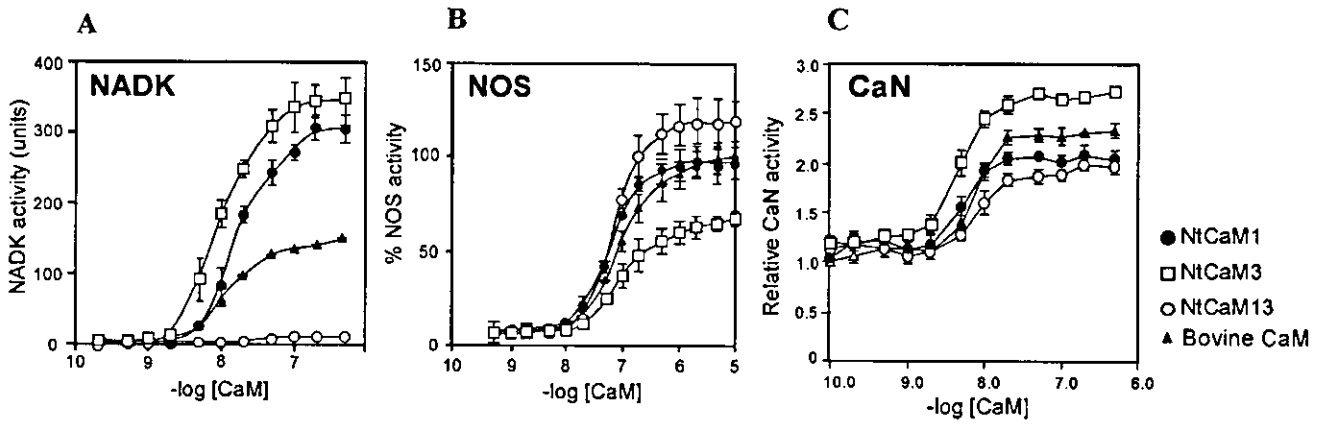

Fig. 2 CaM concentration-dependent activation of three target enzymes. (A) NADK activity was determined by the procedure of Harmon et al. (1984) using NADK purified from pea seedlings with 1 mM Ca^{2+} and increasing NtCaM1 (filled circles), NtCaM3 (open squares), NtCaM13 (open circles) and bovine CaM (filled triangles), respectively, under pH 8.0. One unit of the activity is defined as the conversion of 1 nmol of NAD^+ to $NADP^+$ per 1 min. (B) NOS activity was determined by the citrulline method. Recombinant rat neuronal NOS was reacted with 1 mM Ca^{2+} and increasing individual CaMs. The activity is shown as a % relative to that for 10^{-5} M bovine CaM. (C) CaN activity was determined by the procedure of Anthony et al. (1986) using bovine brain CaN with 0.3 mM Ca^{2+} and increasing individual CaMs. The activity is shown relative to basal activity in the absence of any CaM. Values represent the means of three independent experiments, and error bars indicate ±SD.

increased, but not by type III, whose ratio decreased after wounding (Yamakawa et al. 2001). Furthermore, the activation by types I and II was maximized under elevated Ca^{2+} concentrations and decreased pH, which are induced after exposure to various stimuli (Sanders et al. 1999, Lebrun-Garcia et al. 2002, Lecourieux et al. 2002). The activity of animal NO synthase (NOS), which is also activated by plant CaMs in vitro, was highest, moderate and lowest by type III, type I and type II, respectively, indicating the substrate preference of the CaM types.

Results

NADK was activated by NtCaM1 and NtCaM3 but not by NtCaM13

Plant NADK is activated by plant CaMs (Anderson and Cormier 1978, Roberts and Harmon 1992). This study had been conducted using only type II and III CaMs, lacking data on type I CaMs whose structure and expression profiles are different from those of types II and III (Takezawa et al. 1995, Yamakawa et al. 2001). To understand the role of each CaM type in NADK activation, we used representatives of all three plant-specific CaMs (NtCaM1, 3 and 13) and a control animal CaM (bovine brain CaM). Using purified pea NADK as the target enzyme, we assessed which type of CaM is the most potent activator under conditions of 1 mM Ca^{2+} and pH 8.0. NADK activity was evaluated by quantification of the product, $NADP^+$, via reaction with excess $NADP^+$-dependent glucose 6-phosphate dehydrogenase and oxidation–reduction indicator dyes as described previously (Harmon et al. 1984). Pea NADK was activated most by NtCaM3 and then by NtCaM1 in the presence of 1 mM Ca^{2+} at pH 8.0, but NtCaM13 hardly activated the enzyme (Fig. 2A). Mammalian CaM had less activity than NtCaM1 and 3. In the absence of Ca^{2+}, no activity was detected for any of the CaMs (data not shown). V_{max}, the maximal activity compared with that of the mammalian CaM, and K_{act}, the concentration of CaM required for half-maximal activity, were 207%, 235% and 9%, and 16, 9 and 26 nM for NtCaM1, NtCaM3 and NtCaM13, respectively (Table 1).

NOS was effectively activated by NtCaM13 and then by NtCaM1, but weakly by NtCaM3

NOS is an important CaM-dependent enzyme in animals. We studied the properties of tobacco CaMs using a rat recombinant NOS as a target enzyme according to the citrulline method coupled with thin-layer chromatography (TLC) separation (Kumar et al. 1999). NOS was activated by all tobacco CaM types as well as by mammalian CaM (Fig. 2B). Compared with the control animal CaM, NtCaM13 was the most potent activator, NtCaM1 was the second most potent, while NtCaM3 was the weakest. Without Ca^{2+}, no NOS activity was observed (data not shown). V_{max} compared with that for bovine CaM and K_{act} for NtCaM1, NtCaM3 and NtCaM13 were 98%, 67% and 119%, and 56, 89 and 67 nM, respectively (Table 1).

Calcineurin was most activated by NtCaM3 and moderately activated by NtCaM1 and NtCaM13

Calcineurin (CaN), a CaM-dependent protein phosphatase, is a target of CaM in mammals. The activity of bovine brain CaN was determined by a fluorometric method using 4-methyl umbelliferyl phosphate (4MUP) as the substrate (Anthony et al. 1986). In the absence of Ca^{2+}, the enzyme exhibited 35–45% of the activity in the presence of Ca^{2+} (data not shown). With Ca^{2+}, NtCaM3 increased the activity of bovine CaN 2.7-fold, followed second by bovine CaM, and fol-

Table 1 Activation profiles of NADK, NOS and CaN by NtCaM1, 3, 13 and bovine CaM

	NADK		NOS		CaN	
Target enzyme	V_{max} (%)		V_{max} (%)		V_{max} (%)	
NtCaM1	207	++++	98	++	81	+
NtCaM3	235	+++++	67	+	130	+++
NtCaM13	9	±	119	+++	74	+
Bovine CaM	100	++	100	++	100	++

The extent of activation was summarized. The number of (+) indicates the extent of activation and (±) denotes little activation. V_{max}, the maximal activity compared with that of bovine CaM.

lowed by NtCaM1 and NtCaM13 (Fig. 2C). V_{max} compared with that for bovine CaM and K_{act} for NtCaM1, NtCaM3 and NtCaM13 were 81%, 130% and 74% and 4.6, 4.0 and 7.5 nM, respectively (Table 1).

The Ca^{2+} concentration required for NADK activation is different for different types of CaMs

NADK activation as shown in Fig. 2A was analyzed under similar conditions as described previously (Harmon et al. 1984, Lee et al. 1995); at 1 mM Ca^{2+} and pH 8.0, which is different from real cytosolic conditions found in plant cells. The cytosolic Ca^{2+} concentration ($[Ca^{2+}]_{cyt}$) is around 0.1 μM in unstimulated cells, but dynamically increases as a result of stimuli such as red light, touch, heat shock, oxidative stress, hormonal signals. For instance, $[Ca^{2+}]_{cyt}$ transiently rises to 3 μM after elicitor treatment in suspensison-cultured cells (Sanders et al. 1999, Lecourieux et al. 2002). To understand the Ca^{2+}-dependent activation of NADK by each CaM type in intact plant cells after stimulation, we used the three representative tobacco CaM proteins at various Ca^{2+} concentrations. Because the cytosolic pH in unstimulated plant cells is around 7.5 (Kurkdjian and Guern 1989), the pH of the reaction mixture for this study was adjusted to 7.5. CaM concentration in this study was fixed at 0.5 μM. Although there are few reports on cytosolic CaM concentration in plant, it is said to be 5–20 μM (reviewed by Zielinski 1998). While 0.5 μM CaM is lower than the known concentration, it seemed to be sufficient because NADK activation was saturated at 0.5 μM CaM in Fig. 2A. Under this condition, NtCaM3 could activate NADK at a Ca^{2+} concentration lower than 1 μM (Fig. 3A). However, NtCaM1 required at least 10 μM Ca^{2+}, and its activating ability reached to the same or a higher degree than that of NtCaM3 at 100 μM Ca^{2+}. NtCaM13 could not activate NADK at any Ca^{2+} concentration.

Ca^{2+}-dependent NADK activation is regulated by pH

Next, we examined the effect of pH on NADK activation by CaMs because cytosolic pH is changed by stress such as elicitor treatment. In *N*-acetylchitooligosaccharide elicitor-treated suspension-cultured rice cells, cytosolic pH changed rapidly from 7.5 to 7.1 (Kuchitsu et al. 1997), and the pH declined to 6.8 from 7.3, 40 min after treatment with 0.3 M NaCl in suspension-cultured tobacco cells (Qiao et al. 2002). Thus it is possible that cytosolic pH decreases after stimuli in vivo. To reproduce the actual cytosolic conditions present after stimuli in plants, we used reaction mixtures at pH 7.1, 6.8 and 6.4 with various Ca^{2+} concentrations for the analysis of NADK activation by CaMs. Under pH 7.1, NtCaM1 and 3 activated NADK more efficiently than under pH 7.5 (Fig. 3B). NtCaM3 activated it under pH 7.1 at Ca^{2+} concentrations such as 0.1 μM, and NtCaM1 responded to 1 μM Ca^{2+}, at which NADK activation was not detected under pH 7.5. At pH 6.8, NtCaM3 activation was more efficient than at pH 7.1. NtCaM1 activated NADK similarly to pH 7.1 for almost the same Ca^{2+} concentrations (Fig. 3C). Under pH 6.4, for which the cytosolic pH was changed from 7.3 after NaCl treatment in suspension-cultured tobacco cells to induce cell death (Qiao et al. 2002), the activating ability of both types of CaMs declined (Fig. 3D).

Discussion

In contrast to the mammalian system in which only one CaM protein operates, plants have multiple types of CaMs with different protein structures to transduce Ca^{2+} signals downstream. Using purified NtCaM1, 3 and 13, which belong to plant-specific type I, II and III CaMs, respectively, we analyzed the roles of each type of CaM in target enzyme activation in vitro. Our work presents comparable studies of all three types of plant CaMs and the control animal CaM under experimental conditions mimicking that in the cytosol of healthy unstimulated and stimulated cells. The characterization of type I CaM using NtCaM1 as a representative in comparison with other types of CaMs was first reported in this work, which found that NtCaM1 activates NADK only under stress-induced conditions. From this study, we could understand that the mode of target enzyme activation is different and specific for each type of CaM.

Studies on plant NADK activation by the three types of CaMs under various Ca^{2+} concentrations and pHs gave us important information on the specificity of CaM. Increased Ca^{2+} concentration after stimuli enhanced NADK activation by NtCaM1 and 3, but no activation by NtCaM13 occurred. Similarly, lowered pH after stimuli also enhanced activation by the NtCaM1 and 3, but no activation by NtCaM13 occurred. In

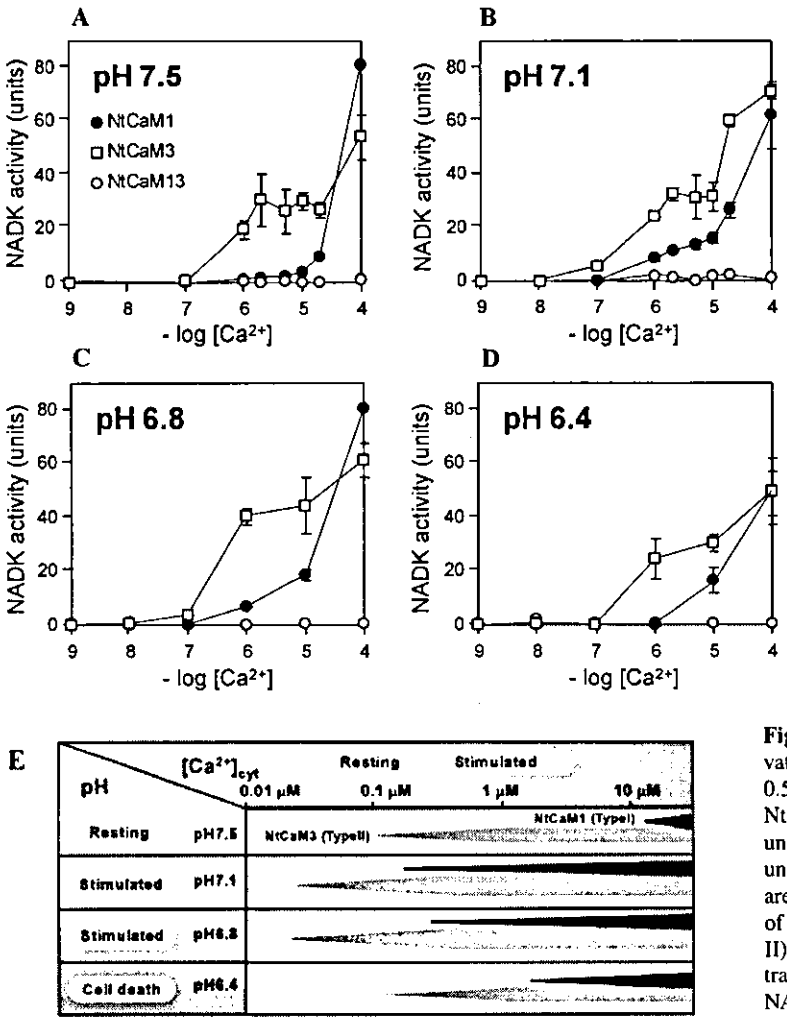

Fig. 3 Effects of Ca^{2+} concentration and pH on NADK activation by NtCaM1, 3 and 13. The assay was conducted with 0.5 µM NtCaM1 (filled circles), NtCaM3 (open squares) and NtCaM13 (open circles), respectively, and increasing Ca^{2+} under pH 7.5 (A), pH 7.1 (B), pH 6.8 (C) or pH 6.4 (D). One unit of the NADK activity is the same as in Fig. 2. The data are the mean of at least two experiments ±SD. (E) Illustration of NADK activation by NtCaM1 (type I) and NtCaM3 (type II). The activity was enhanced under increased Ca^{2+} concentration and decreased pH. Crescendo bars indicate the level of NADK activity.

contrast, NtCaM13 most effectively activated another target enzyme, NOS. These results indicate that plants efficiently use three types of CaMs to activate different target enzymes adapted for the circumstances induced by various stimuli.

$[Ca^{2+}]_{cyt}$ in plant cells at steady state is around 0.1 µM (Bush 1995). After stress treatment such as elicitor application (Lecourieux et al. 2002) and pathogen infection (Xu and Heath 1998), $[Ca^{2+}]_{cyt}$ increases, triggering stress-responsive signaling pathways used for self-defense. Cytosolic pH is also dynamically altered to bring about acidification after stress treatment (Kurkdjian and Guern 1989). This evidence suggests that Ca^{2+}-induced target enzyme activation in vitro should be studied under similar conditions in unstimulated and stimulated plant cells in vivo to obtain meaningful data. We examined Ca^{2+}/CaM-dependent NADK activation under conditions mimicking the cytosolic conditions of plant cells before and after stimuli.

We found that plant NADK was more effectively activated by type I and II NtCaMs under pH 7.1 and 6.8, which are stress-inducible cytosolic pHs, than at pH 7.5, which is the cytosolic pH in unstimulated plant cells. A report by Yamamoto (1966) showed that in crude green leaf extract, NADK activity was highest at pH 6.8 when reacted in buffer at pH 5.2–8.4, which supports our findings. Furthermore, we found that NtCaM3 could activate NADK at Ca^{2+} concentrations between 0.1 and 1 µM at all pH values tested. Since the $[Ca^{2+}]_{cyt}$ in plant cells at steady state is around 0.1 µM (Bush 1995), NADK activation by type II CaMs would occur constitutively and is enhanced by increased Ca^{2+} after stimuli, indicating that type II CaMs respond most sensitively to small stimuli. In contrast to type II CaMs, wound-inducible type I CaMs such as NtCaM1 did not respond to Ca^{2+} concentration lower than 1 µM but did to Ca^{2+} higher than 10 µM at pH 7.5, implying that type I CaMs do not function in NADK activation in healthy unstimulated cells. Since NtCaM1 responded to low Ca^{2+} concentrations such as 1 µM at pH 7.1 and 6.8 but not at pH 7.5, it appears that type I CaMs are recruited only in stimu-

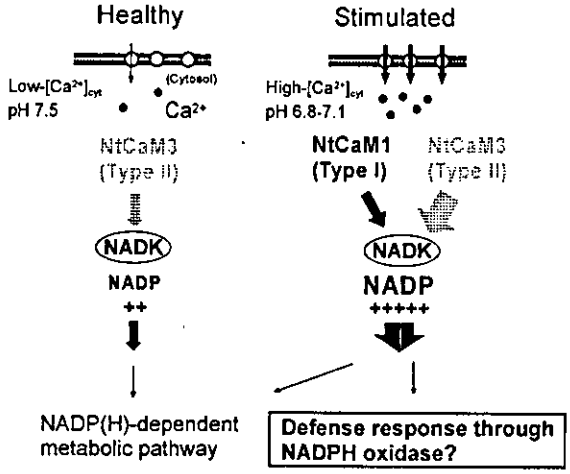

Fig. 4 Hypothetical model of NADK activation in plant cells. Left, an unstimulated healthy cell in which only NtCaM3 activates NADK conferring NADP(H)-dependent metabolic pathway. Right, a stimulated cell, in which NtCaM3 is further activated and NtCaM1 is newly potentiated for NADK activation by elevated Ca^{2+} concentration and decreased pH, likely enhancing the defense response through NADPH oxidase.

lated cells in which $[Ca^{2+}]_{cyt}$ has increased and pH has declined (Fig. 3E).

Many reports indicated the involvement of CaMs in plant self-defense responses (Heo et al. 1999, Kim et al. 2002). A transgenic tobacco plant that possesses a mutated CaM, which contains one amino acid substitution crucial for the hyperactivation of NADK, showed enhanced H_2O_2 production in response to elicitor treatment (Harding et al. 1997). Since ROS such as H_2O_2 are produced by NADPH oxidase activity, these CaMs likely promote the production of its substrate $NADP^+$/NADPH by activating NADK to convert NAD^+ to $NADP^+$. In suspension-cultured tobacco cells treated with cryptogein, a phytopathogenic fungus-derived proteinous elicitor, the pentose phosphate pathway is activated, which enhances $NADP^+$/NADPH conversion (Pugin et al. 1997). The production of O_2^- by tobacco homologs of NADPH oxidase is stimulated by TMV infection and Ca^{2+} application (Sagi and Fluhr 2001). At low $[Ca^{2+}]_{cyt}$ in unstimulated cells, only type II CaMs such as NtCaM3 would activate NADK, producing a basal level of NADP(H) almost all of which is consumed by reducing reactions such as photosynthesis in plant cells. When $[Ca^{2+}]_{cyt}$ increases and pH decreases due to a stimulus, NtCaM1 and NtCaM3 may activate NADK more effectively in elevating the NADP(H) level, making available excess NADP(H) for the NADPH oxidase reaction to produce ROS. Thus, type I CaMs including NtCaM1 may trigger Ca^{2+} signaling for ROS production after stimulation such as by wounding or elicitor treatment (Fig. 4).

Generally, plant CaMs have four sets of well-conserved EF-hand motifs for Ca^{2+} binding. The reason for three types of tobacco CaMs with different abilities to activate NADK at different Ca^{2+} concentration is a focus of interest. As for plant NADK activation by CaM, it was reported that Lys-30 and Gly-40 in the first EF-hand of soybean SCaM-1, which is the ortholog of NtCaM3, are essential for NADK activation but not for binding to the enzyme. Soybean SCaM-4, which is the ortholog of NtCaM13 and has Glu-30 and Asp-40, does not activate NADK but can bind to the enzyme (Lee et al. 1997). Consistent with this, both NtCaM1 and 3 have Lys-30 and Gly-40 in the first EF-hand, whereas NtCaM13 has Glu-30 and Asp-40(Fig. 1A). This evidence indicates that the difference in these amino acids is not involved in the difference in Ca^{2+} response between NtCaM1 and NtCaM3. Liao et al. (1996) suggested that the C-terminal hydrophobic region of CaM plays a role in binding to several target proteins including NADK. Since NtCaM1 has a different amino acid sequence from that of NtCaM3 in the C-terminal region rather than around EF-hands (Fig. 1A), different Ca^{2+} responses for NADK activation may be attributed to the predicted difference in binding affinity between Ca^{2+}/CaM and NADK rather than the affinity between Ca^{2+} and CaM.

In contrast to plant NADK, mammalian NOS was most activated by NtCaM13 (Fig. 2C). Ca^{2+}-dependent NOS-like activity is necessary for the expression of pathogenesis-related (*PR*) genes following TMV infection in tobacco plants (Durner et al. 1998). We confirmed the results of Heo et al. (1999) for the constitutive expression of *PR* genes in transgenic tobacco plants overproducing NtCaM13/SCaM-4-type CaMs (unpublished data). Thus, type III CaMs might regulate *PR* gene expression involved in the defense response against pathogen infection by an unknown mechanism. Recently, Chandok et al. (2003) indicated that a variant of the P protein of glycine decarboxylase had NOS activity, and that it is induced by viral infection. Another study revealed that an *Arabidopsis* NOS gene encodes a protein with sequence similarity to a NO synthesis-related protein in the snail *Helix pomatia* (Guo et al. 2003). The evaluations of plant NOS enzymes reported so far and the isolation of new putative plant NOS molecules as CaM binding proteins will help in the elucidation of Ca^{2+}/CaM signaling during self-defense reactions in plants.

At present, genes of the target enzymes of tobacco CaMs in self-defense signaling to pathogen infection and wounding have not been identified. One of the candidates is a putative tobacco MAPK phosphatase (NtMKP1) which we isolated as a CaM binding protein (Yamakawa et al. 2004). Wound-induced activation of defense-related MAPKs such as WIPK and SIPK was significantly inhibited in transgenic tobacco plants overproducing NtMKP1, indicating that the MAPK phosphatase is involved in MAPK signaling via a Ca^{2+}/CaM system after wounding or pathogen infection. NtMKP1 has higher binding affinity to NtCaM1 and NtCaM3 than to NtCaM13. An amino acid substitution in the CaM binding domain of NtMKP1 abolished NtCaM1 and NtCaM3 binding. The structure of NtMKP1 is considerably different from that of animal MKPs, suggesting that plants have specific Ca^{2+}/CaM signaling cascades via

the MKP/MAPK system which are quite different from those of animals.

Plants lack the highly developed immune system that vertebrates have, and vertebrates have only one CaM protein with an identical amino acid sequence. Our data suggest that transcriptional and post-transcriptional control of diverse plant CaM isoforms with a characteristic manner may effectively activate individual target enzymes and transduce the Ca^{2+} signal downstream via dynamic changes in cytosolic Ca^{2+} concentration and pH upon internal and external stimulation. The isolation and characterization of other plant-originated target molecules of individual CaMs by direct analysis of CaM-interacting proteins will shed light on the physiological importance of individual CaM isoforms for the self-defense mechanism in plants.

Materials and Methods

Purification of CaM protein

Recombinant CaM proteins NtCaM1, 3 and 13 were produced by *Escherichia coli* harboring pET-NtCaM1, 3 and 13, respectively, and purified by Ca^{2+}-dependent hydrophobic chromatography as described previously (Fromm and Chua 1992, Yamakawa et al. 2001). As shown in Fig. 1B, the purity of CaM proteins that showed an electrophoretic mobility shift in the presence of Ca^{2+} was >95% as seen by Coomassie Brilliant Blue (CBB) staining following separation on SDS–polyacrylamide gel. Bovine brain CaM was obtained from Wako (Osaka, Japan), and used as a control for the enzyme assays. Protein concentration was determined by both the Bradford method (Bradford 1976) and the Lowry method (Lowry et al. 1951) using a protein assay kit (Bio-Rad, Hercules, CA, U.S.A.) with BSA as the standard.

Purification of NADK

Pea NADK was partially purified from pea seedlings (*Pisum sativam* L. cv. Akabana-tsurunashi-endo) by the method of Muto and Miyachi (1977). Peas were germinated in moistened vermiculite and grown under artificial light without additional nutrients. The following purification procedures were carried out at 4°C. The aerial parts of 12-day-old seedlings (627 g) were macerated with liquid nitrogen and extracted with 3 vol of 25 mM triethanolamine-acetate (pH 7.5) containing 1 mM phenylmethylsulfonyl fluoride, 0.5 M sucrose and 1 mM DTT. The homogenate was squeezed through double-layered Miracloth (Calbiochem, La Jolla, CA, U.S.A.) and centrifuged at 27,000×*g* for 30 min. A one-tenth volume of 0.7% protamine sulfate solution in 10 mM triethanolamine-acetate buffer (pH 7.5) was added to the supernatant (2,000 ml). After continuous stirring for 15 min, the precipitate was collected by centrifugation at 27,000×*g* for 15 min. From the precipitate, the enzyme was extracted with 250 ml of 0.2 M Na-acetate buffer (pH 6.0) and 1 μg ml^{-1} pepstatin A. To the extract, the same volume of 50% (w/w) polyethylene glycol 6,000 solution was added and the mixture was stirred for 30 min. After centrifugation at 39,000×*g* for 30 min, the precipitate was resuspended in 100 ml of 50 mM Tris–HCl (pH 7.0), 100 mM KCl, 3 mM $MgCl_2$ and 1 mM EGTA. Insoluble materials were removed by centrifugation at 27,000×*g* for 15 min. The supernatant solution was passed through a DEAE–Sephacel (Amersham Pharmacia Biotech, Buckinghamshire, UK) column (1.6×30 cm) pre-equilibrated with the buffer mentioned above, allowing pea endogenous CaM to be completely adsorbed by the column. The effluent was stocked at –80°C in small portions of 5% glycerol solution and used for NADK assays.

NADK assay

The NADK assay was performed as described previously (Harmon et al. 1984) in a 0.5-ml solution A containing 50 mM Tricine (pH 8.0), 5 mM $MgCl_2$, 2 mM NAD^+, 3 mM ATP, 1 mM $CaCl_2$ or EGTA and various amounts of CaM. The reaction was initiated with 10 μl of freshly thawed, purified NADK stock solution. After incubation for 60 min at 37°C, the reaction was terminated by placing the tubes in boiling water for 3 min. The tubes were then cooled to ambient temperature, and 0.5 ml of solution B containing 50 mM Tricine (pH 8.0), 5 mM $MgCl_2$, 1 mM EGTA, 0.8 mM glucose 6-phosphate, 0.1 mg ml^{-1} phenazine methosulfate, and 0.15 mg ml^{-1} 2,6-dichlorophenolindophenol was added. The mixture was transferred to a cuvette pre-incubated at 30°C, and 20 μl of glucose 6-phosphate dehydrogenase (6 U ml^{-1}) was added. The decrease in A_{600} per minute was monitored using a Beckman spectrophotometer (Model DU-7400; Fullerton, CA, U.S.A.) equipped with a temperature controller set at 30°C. The amount of $NADP^+$ produced by the NADK reaction was calculated from a standard curve of $NADP^+$ versus the descending rate of A_{600}. No activation by Ca^{2+} was found in the absence of exogenous CaM, confirming that the preparation of NADK was free from contamination by pea endogenous CaM (data not shown). To analyze the effect of Ca^{2+} concentration and pH, solutions of CaM and NADK were dialyzed respectively against 50 mM Tris–HCl (pH 7.5), 3mM $MgCl_2$. Solution C, which contained various amounts of $CaCl_2$ buffered by BAPTA, 50 mM PIPES (pH7.5, 7.1, 6.8, 6.4), 5 mM $MgCl_2$, 2 mM NAD^+, 3 mM ATP, 0.5 μM CaM was used in place of solution A. Since concentration of free Ca^{2+} is depending on pH or other components such as Mg^{2+} and ATP, we previously used calculation software (BOUND AND DETERMINED; Brooks and Storey 1992) for determination of $CaCl_2$ and BAPTA concentrations in solution C.

NOS assay

NOS activity was determined by the citrulline assay followed by TLC, as described by Kumar et al. (1999). The freshly prepared reaction mixture (20 μl) consisted of 30 mM HEPES–NaOH (pH 7.0), 2 mM NADPH, 100 μM FAD, 100 μM tetrahydrobiopterin, 1 mM $CaCl_2$ or EGTA, various concentrations of CaM, 0.25 μl of L-[U-^{14}C]arginine (272 mCi $mmol^{-1}$, 100 μCi ml^{-1}; Moravek Biochemicals, Brea, CA, U.S.A.) and 100 mU of recombinant rat neuronal NOS (Calbiochem). The reaction was carried out at 30°C for 60 min. The NOS reaction was terminated by adding 50 μl of cold methanol. The samples were left on ice for 20 min and centrifuged at 20,000×*g* for 10 min. An aliquot (10 μl) of the supernatant was spotted onto a silica gel TLC plate (Merck, Darmstadt, Germany), air-dried and subjected to chromatography. The solvent was ammonium hydroxide:chloroform:methanol:water (4 : 1 : 9 : 2). The plate was imaged by a PhosphorImager SI (Amersham Pharmacia Biotech) after exposure for 48 h and the radioactivity of the product, L-[^{14}C]citrulline, was quantified using the ImageQuant 1.1 program (Amersham Pharmacia Biotech). The R_f values for L-arginine and L-citrulline were 0.44 and 0.90, which were those of the standard amino acids stained with ninhydrin (data not shown).

Calcineurin assay

The activity of a CaM-dependent protein phosphatase, CaN, was determined by a fluorescent assay using 4-MUP (ICN, Costa Mesa, CA, U.S.A.) as the substrate, as reported previously (Anthony et al. 1986). Each assay was conducted in 200 μl of 50 mM Tris–HCl (pH 8.0), 1 mg ml^{-1} BSA, 0.5 mM DTT, 1 mM $MgCl_2$, 0.3 mM $CaCl_2$ or EGTA, 12.5 nM bovine brain CaN (Upstate Biotechnology, Lake Placid, NY, U.S.A.), with various concentrations of CaM, and 200 μM 4MUP, which was added to start the reaction. After incubation at 37°C for 60 min, the reaction was terminated by the addition of 1 ml of 0.4

M Na_2CO_3. Fluorescence was monitored in a quartz cuvette (1 cm light path) using a Hitachi fluorescence spectrophotometer (Model F-2500; Tokyo, Japan) with an excitation wavelength of 365 nm and an emission wavelength of 446 nm. To correlate the amount of product, 4-methyl umbelliferone (4MU), with the amount of fluorescence, a standard curve was made by monitoring the fluorescence intensity as a function of the concentration of 4MU. All assays were corrected for the non-enzymic hydrolysis of 4MUP. Specific activity was defined as nmol 4 MU mg^{-1} min^{-1}.

Acknowledgments

We thank Drs S. Seo, K. Higashi, S. Katou and Ms Y. Gotoh for helpful advice regarding procedures. This work was supported in part by grants from the COE (Center of Excellence) project and a Grant-in-aid for scientific research on the Molecular Mechanisms of Plant–Pathogenic Microbe Interaction,from the Ministry of Education, Science and Culture, Japan.

References

Anderson, J.M. and Cormier, M.J. (1978) Calcium-dependent regulator of NAD kinase in higher plants. *Biochem. Biophys. Res. Commun.* 84: 595–602.

Anthony, F.A., Merat, D.L. and Cheung, W.Y. (1986) A spectrofluometric assay of calmodulin-dependent protein phosphatase using 4-methylumbelliferyl phosphate. *Anal. Biochem.* 155: 103–107.

Bradford, M.M. (1976) A rapid and sensitive method for the quantitation of microgram quantities of protein utilizing the principle of protein–dye binding. *Anal. Biochem.* 72: 248–254.

Brooks, S.P.J. and Storey, K.B. (1992) Bound and determined: a computer program for making buffers of defined ion concentrations. *Anal. Biochem.* 201: 119–126.

Bush, D.S. (1995) Calcium regulation in plant cells and its role in signaling. *Annu. Rev. Plant Mol. Biol.* 46: 95–122.

Chandok, M.R., Ytterberg, A.J., Van Wijk, K.J. and Klessig, D.F. (2003) The pathogen-inducible nitric oxide synthase (iNOS) in plants is a variant of the P protein of the glycine decarboxylase complex. *Cell* 113: 469–482.

Cho, M.J., Vaghy, P.L., Kondo, R., Lee, S.H., Davis, J.P., Rehl, R., Heo, W.D. and Johnson, J.D. (1998) Reciprocal regulation of mammalian nitric oxide synthase and calcineurin by plant calmodulin isoforms. *Biochemistry* 37: 15593–15597.

Delledonne, M., Xia, Y., Dixon, R.A. and Lamb, C. (1998) Nitric oxide functions as a signal in plant disease resistance. *Nature* 394: 585–588.

Durner, J., Wendehenne, D. and Klessig, D.F. (1998) Defense gene induction in tobacco by nitric oxide, cyclic GMP, and cyclic ADP-ribose. *Proc. Natl Acad. Sci. USA* 95: 10328–10333.

Fromm, H. and Chua, N.-H. (1992) Cloning of plant cDNAs encoding calmodulin-binding proteins using ^{35}S-labeled recombinant calmodulin as a probe. *Plant Mol. Biol. Rep.* 10: 199–206.

Grant, M., Brown, I., Adams, S., Knight, M., Ainslie, A. and Mansfield, J. (2000) The *RPM1* plant disease resistance gene facilitates a rapid and sustained increase in cytosolic calcium that is necessary for the oxidative burst and hypersensitive cell death. *Plant J.* 23: 441–450.

Goodman, R.N. and Novacky, A.J. (1994) The hypersensitive reaction in plants to pathogens. APS Press, St. Paul, Minnesota, U.S.A.

Guo, F.Q., Okamoto, M. and Crawford, N.M. (2003) Identification of a plant nitric oxide synthase gene involved in hormonal signaling. *Science* 302: 100–103.

Hahlbrock, K., Scheel, D., Logemann, E., Nürnberger, T., Parniske, M., Reinold, S., Sacks, W.R. and Schmelzer, E. (1995) Oligopeptide elicitor-mediated defense gene activation in cultured parsley cells. *Proc. Natl Acad. Sci. USA* 92: 4150–4157.

Harding, S.A., Oh, S.-H. and Roberts, D.M. (1997) Transgenic tobacco expressing a foreign calmodulin gene shows an enhanced production of active oxygen species. *EMBO J.* 16: 1137–1144.

Harmon, A.C., Jarrett, H.W. and Cormier, M.J. (1984) An enzymatic assay for calmodulins based on plant NAD kinase activity. *Anal. Biochem.* 141: 168–178.

Heo, W.D., Lee, S.H., Kim, M.C., Kim, J.C., Chung, W.S., Chun, H.J., Lee, K.J., Park, C.Y., Park, H.C., Choi, J.Y. and Cho, M.J. (1999) Involvement of specific calmodulin isoforms in salicylic acid-independent activation of plant disease resistance responses. *Proc. Natl Acad. Sci. USA* 96: 766–771.

Kadota, Y., Goh, T., Tomatsu, H., Tamauchi, R., Higashi, K., Muto, S. and Kuchitsu, K. (2004) Cryptogein-induced initial events in tobacco BY-2 cells: pharmacological characterization of molecular relationship among cytosolic Ca^{2+} transients, anion efflux and production of reactive oxygen species. *Plant Cell Physiol.* 45: 160–170.

Kim, M.C., Panstrugua, R., Elliott, C., Muller, J., Devoto, A., Yoon, H.W., Park, H.C. Cho, M.J. and Schulze-Lefert, P. (2002) Calmodulin interacts with MLO protein to regulate defence against mildew in barley. *Nature* 416: 447–450.

Klee, C.B. and Vanaman, T.C. (1982) Calmodulin. *Adv. Protein Chem.* 35: 213–321.

Kuchitsu, K., Yazaki, Y., Sakano, K. and Shibuya, N. (1997) Transient cytoplasmic pH change and ion fluxes through the plasma membrane in suspension-cultured rice cells triggered by *N*-acetylchitooligosaccharide elicitor. *Plant Cell Physiol.* 38: 1012–1018.

Kumar, V.B., Bernardo, A.E., Alshaher, M.M., Buddhiraju, M., Purushothaman, R. and Morley, J.E. (1999) Rapid assay for nitric oxide synthase using thin-layer chromatography. *Anal. Biochem.* 269: 17–20.

Kurkdjian, A. and Guern, J. (1989) Intercellular pH: measurement and importance in cell activity. *Annu. Rev. Plant Mol. Biol.* 40: 271–303.

Lebrun-Garcia, A., Chiltz, A., Gout, E., Bligny, R. and Pugin, A. (2002) Questioning the role of salicylic acid and cytosolic acidification in mitogen-activated protein kinase activation induced by cryptogein in tobacco cells. *Planta* 214: 792–797.

Lecourieux, D., Mazars, C., Pauly, N., Ranjeva, R. and Pugin, A. (2002) Analysis and effects of cytosolic free calcium increases in response to elicitors in *Nicotiana plumbaginifolia* cells. *Plant Cell* 14: 2627–2641.

Lee, S.H., Kim, J.C., Lee, M.S., Heo, W.D., Seo, H.Y., Yoon, H.W., Hong, J.C., Lee, S.Y., Bahk, J.D., Hwang, I. and Cho, M.J. (1995) Identification of a novel divergent calmodulin isoform from soybean which has differential ability to activate calmodulin-dependent enzymes. *J. Biol. Chem.* 270: 21806–21812.

Lee, S.H., Seo, H.Y., Kim, J.C., Heo, W.D., Chung, W.S., Lee, K.J., Kim, M.C., Cheong, Y.H., Choi, J.Y., Lim, C.O. and Cho, M.J. (1997) Differential activation of NAD kinase by plant calmodulin isoforms: the critical role of domain I. *J. Biol. Chem.* 272: 9252–9259.

Liao, B., Gawienowski, M.C. and Zielinski, R.E. (1996) Differential stimulation of NAD kinase and binding of peptide substrates by wild-type and mutant plant calmodulin isoforms. *Arch. Biochem. Biophys.* 327: 53–60.

Lowry, O.H., Rosebrough, N.J., Farr, A.L. and Randall, R.J. (1951) Protein measurement with the folin phenol reagent. *J. Biol. Chem.* 193: 265–275.

Muto, S. and Miyachi, S. (1977) Properties of a protein activator of NAD kinase from plants. *Plant Physiol.* 59: 55–60.

Niki, T., Mitsuhara, I., Seo, S., Ohtsubo, N. and Ohashi, Y. (1998) Antagonistic effect of salicylic acid and jasmonic acid on the expression of pathogenesis-related (PR) protein genes in wounded mature tobacco leaves. *Plant Cell Physiol.* 39: 500–507.

Nürnberger, T., Nennstiel, D., Jabs, T., Sacks, W.R., Hahlbrock, K. and Scheel, D. (1994) High affinity binding of a fungal oligopeptide elicitor to parsley plasma membranes triggers multiple defense response. *Cell* 78: 449–460.

Park, H.-J., Miura, Y., Kawakita, K., Yoshioka, H. and Doke, N. (1998) Physiological mechanisms of a sub-systemic oxidative burst triggered by elicitor-induced local oxidative burst in potato tuber slices. *Plant Cell Physiol.* 39: 1218–1225.

Pugin, A., Frachisse, J.-M., Tavernier, E., Bligny, R., Gout, E., Douce, R. and Guern, J. (1997) Early events induced by the elicitor cryptogein in tobacco cells: involvement of a plasma membrane NADPH oxidase and activation of glycolysis and the pentose phosphate pathway. *Plant Cell* 9: 2077–2091.

Qiao, J., Mitsuhara, I., Yazaki, Y., Sakano, K., Gotoh, Y., Miura, M. and Ohashi, Y. (2002) Enhanced resistance to salt, cold and wound stress by overproduction of animal cell death suppressors Bcl-xL and Ced-9 in tobacco cells—their possible contribution through improved function of organella. *Plant Cell Physiol.* 43: 992–1005.

Reddy, A.S.N. (2001) Calcium: silver bullet in signaling. *Plant Sci.* 160: 381–404.

Roberts, D.M. and Harmon, A.C. (1992) Calcium-modulated proteins: targets of intracellular calcium signals in higher plants. *Annu. Rev. Plant Physiol. Plant Mol. Biol.* 43: 375–414.